CHARACTERIZATION OF THE NOVEL PROTEIN-PROTEIN INTERACTION BETWEEN GleIF4E2 AND GleIF2β AND ITS BINDING PARTNERS IN TRANSLATION INITIATION

FRANCIS OWUSU KWARTENG

A thesis submitted to the graduate faculty of the College of Arts, Education, and Sciences
at the University of Louisiana Monroe in partial fulfillment of the requirement
for the degree of Master of Science in Biology

May, 2023

Approved by:

Srinivas Garlapati, Ph.D.
Major Professor

Christopher Gissendanner, Ph.D.
Committee Member

Ann Findley, Ph.D.
Committee Member

ACKNOWLEDGMENT

I would like to express my profound gratitude to Dr. Srinivas Garlapati, my esteemed supervisor, for all the guidance, support, and instructions he provided me while working in his lab. I would like to thank Dr. Ann Findley and Dr. Christopher Gissendanner for their guidance throughout my academic journey. In addition, I would like to thank the faculty at the Biology and Pharmacy departments at ULM, who taught and encouraged me during my graduate studies.

I would like to acknowledge and thank my lab mate Zachary Fussell Wiggins whose endless encouragement impacted my work immensely, and Breanna Gottschalck for the support and excellent lab management. I want to give a special thanks to Timothy McMahan and John Neal for the extra help and support.

Finally, I would like to thank my family, Chasity Jones Kwarteng, Harriet Kwarteng, Shadrach Kwarteng, Abigail Kwarteng, Millicent Kwarteng, and Kojo Kwarteng, for always loving and believing in me.

ABSTRACT
Francis Owusu Kwarteng
Characterization of the Novel Protein-Protein Interaction between GleIF4E2 and GleIF2β and its Binding Partners in Translation Initiation
(Major Professor: Srinivas Garlapati, Ph.D.)

Giardia lamblia is a human parasite that causes intestinal diarrheal disease. The parasite shares prokaryotic and eukaryotic characteristics, as seen in its unique translation initiation machinery that does not rely on scanning. Homolog for eIF4G, a scaffold protein that recruits the preinitiation complex onto the mRNA, is absent in *Giardia.* This raises the question of how the preinitiation complex is recruited to the mRNA. To elucidate the molecular mechanism of translation initiation in Giardia, a GST pull-down assay was used to characterize the protein-protein interaction between GleIF4E2 and components of the preinitiation complex. Experimental data from the GST-pull assay confirmed the novel interaction between GleIF4E2 and GleIF2β and several initiation factors within the preinitiation complex. It is proposed that the interaction between GleIF4E2 and GleIF2β is sufficient in recruiting the preinitiation complex through complex and dynamic interactions with other initiation factors, as determined with the pull-down assay.

TABLE OF CONTENTS

LIST OF FIGURES

LIST OF ABBREVIATIONS

eIF	Eukaryotic initiation factor
GleIF	*Giardia lamblia* eukaryotic initiation factor
IF	Initiation Factor
IgG-HRP	Immunoglobulin-Gamma Horseradish Peroxidase
IPTG	Isopropyl ß-D-1-thiogalactopyranoside
IRES	Internal ribosome entry site
LB	Luria Bertani medium
NSF	National Safety Foundation
NTA	Nitrilotriacetic
ORF	Open reading frame
PCR	Polymerase chain reaction
PIC	preinitiation complex
PPI	Protein-protein interaction
PVDF	Polyvinylidene Difluoride
RNA	Ribonucleic acid
SD	Shine Dalgarno
UAS	Upstream Activation Sequence
UTR	Untranslated Region
Y2H	Yeast two-hybrid

CHAPTER I

Literature Review

Giardia lamblia (*G. intestinalis* and *G. duodenalis*) is a flagellated protozoan and obligate gastrointestinal parasite that causes giardiasis (R. D. Adam, 2021). There are eight genetic groups of the parasite termed assemblages A-H. Assemblages A and B cause all human infections. Recent reports indicate assemblage E may also cause human infection (Monis et al., 2009). *Giardia* is the most prevalent cause of diarrheal disease globally. It is estimated to cause symptomatic infection in about 280 million people annually (Ventura et al., 2018).

Most reported cases of giardiasis occur in developing countries with an increased risk of infection due to poverty and poor hygiene (Awasthi & Pande, 1997). Developed countries are not immune to the devastating effects of giardiasis. The disease is commonly associated with traveling to endemic regions and waterborne outbreaks. Higher sanitary standards limit the prevalence of sporadic localized infections. In the United States, *Giardia* is the most common cause of waterborne bouts of diarrhea (Lee et al., 2002). Due to its clinical and epidemiological significance, the WHO included *Giardia* in the 'Neglected Diseases Initiative' in September 2004 (Savioli et al., 2006). Although giardiasis is typically asymptomatic, chronic infection can result in growth retardation and malnutrition in children (Fraser et al., 2000).

Transmission and Epidemiology

Giardia species has two distinct life forms: the vegetative trophozoite is responsible for replication within the host gastrointestinal tract, and the infective cyst is responsible for transmitting the parasite. The infective cyst (Figure 1) can survive harsh environmental conditions. The inert property of the cyst allows it to stay for several months in cold water or soil (CDC, 2013). Infection can occur indirectly when the host ingests water or food contaminated with the cyst or directly from person to person through fecal-oral contact. The infective dose for humans can be as few as ten cysts. Following ingestion of the cyst, localized infection occurs in the intestinal lumen, where the acidic condition of the stomach causes excystation of the cyst—individual cyst release excyzoite, which generates four trophozoites after two rounds of division. The trophozoite (Figure 2) colonizes the upper small intestine using its ventral sucking disk and causes symptoms of diarrhea and malabsorption. It then replicates via asexual binary fission. Some trophozoite encysts after exposure to biliary fluid in the jejunum. This results in the inactive and environmentally resistant cyst form passed in feces. The transmission cycle is complete once the cyst gets outside the host and back into the environment (R. D. Adam, 2021; Ortega & Adam, 1997).

Children in daycare centers, men who have sex with men, backpackers, campers, and travelers to endemic regions are most at risk of *Giardia* infection (Escobedo et al., 2014; Guimarães & Sogayar, 2002). Transmission of giardiasis via drinking and recreational water sources is the most common cause of endemic waterborne gastrointestinal illness (E. A. Adam et al., 2016; Benedict et al., 2017).

Figure 1

Schematic Cartoon of the Giardia Cyst

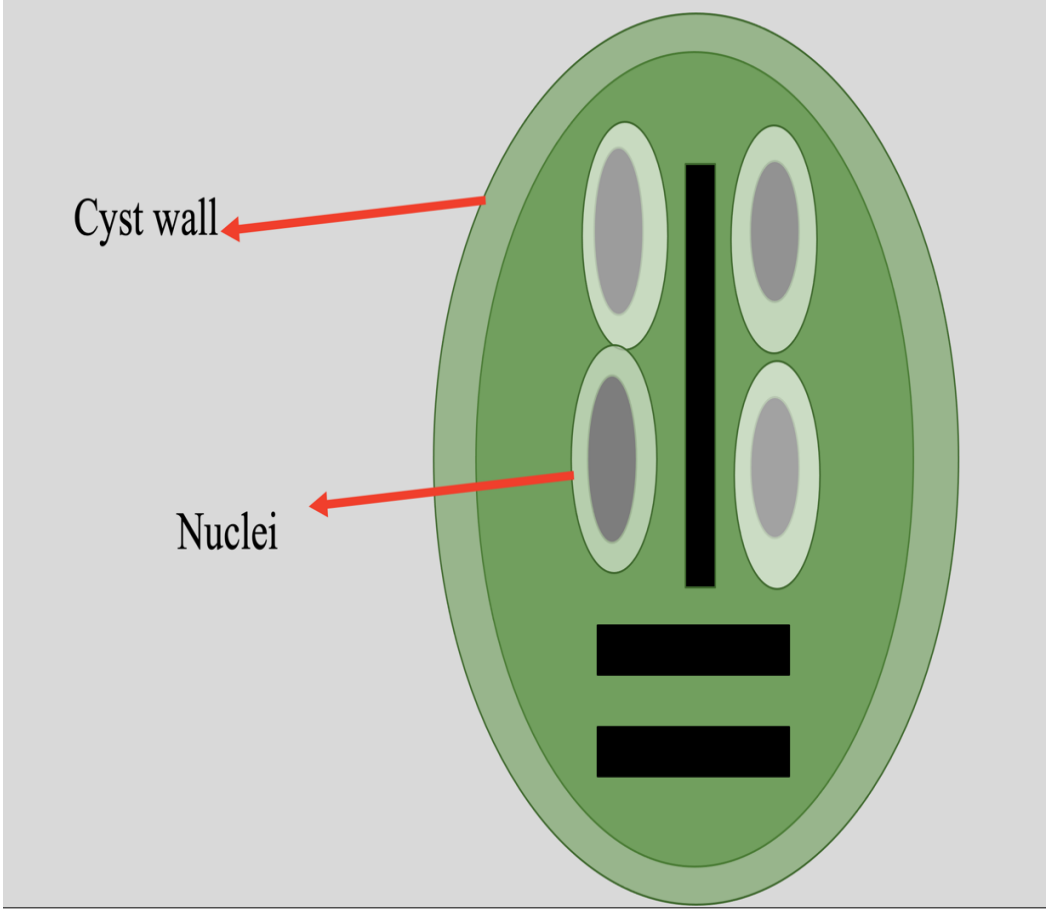

Note. Encystation occurs after nuclear replication, but prior to cytokinesis, this accounts for the four nuclei seen in the infective cyst. Typically, the cyst is about 5 by 7 to 10 µm in diameter and is covered by a wall that comprises a thick outer filamentous layer and an inner membranous layer.

Figure 2

Schematic Cartoon of the Giardia Trophozoite

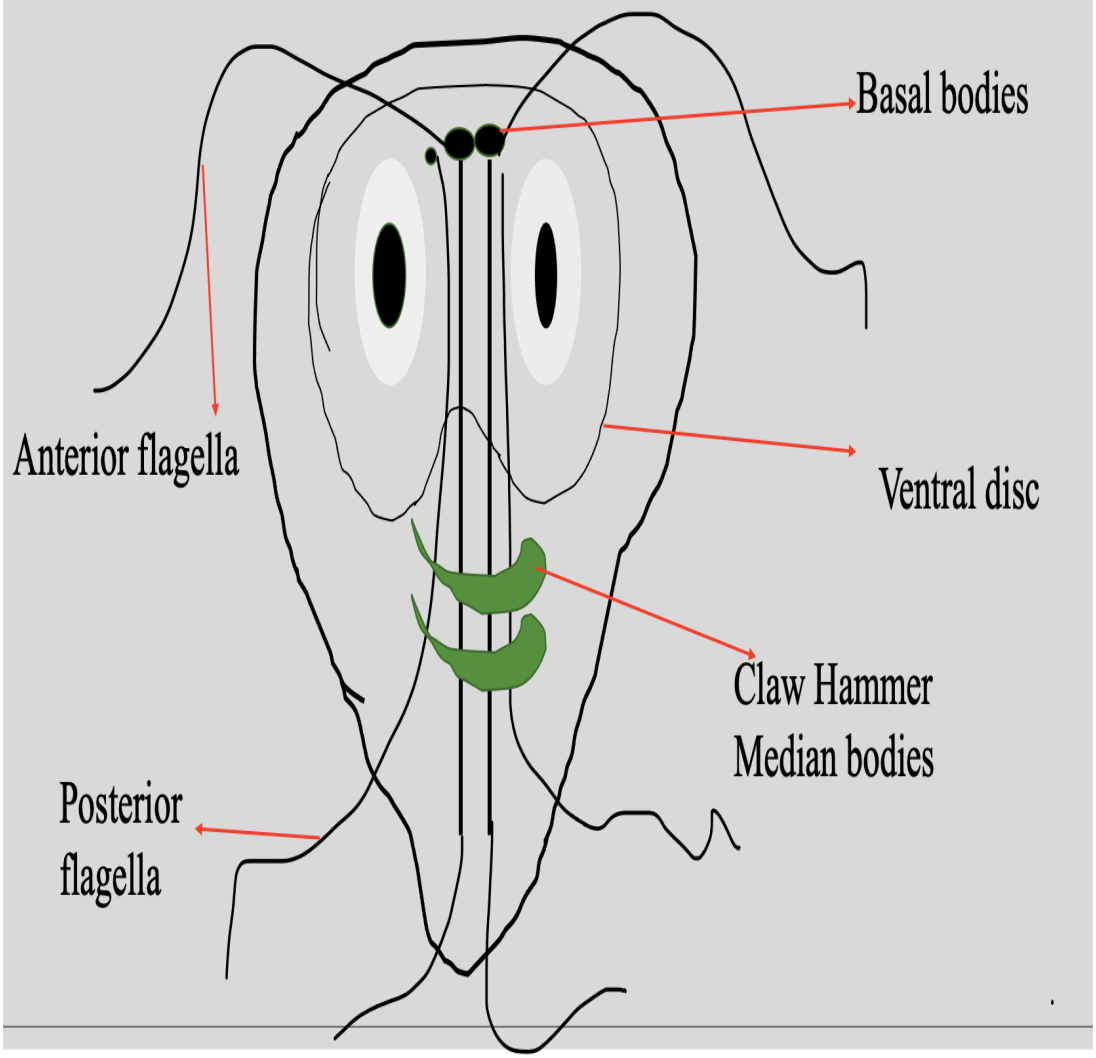

Note. The trophozoite is approximately 12 to 15 µm long and 5 to 9 µm wide. Unlike the cyst, trophozoites have two nuclei without nucleoli.

According to the WHO, middle-income countries, particularly in sub-Saharan Africa, Latin America, and South Asia, have a 20% higher prevalence of giardiasis compared to high-income countries with good sanitary conditions. In first-world countries, the disease is common among individuals with increased risk factors, such as those with HIV/AIDS or undergoing chemotherapy, and marginalized individuals in society who do not have access

to good sanitation and proper hygiene. The high prevalence of transmission through both treated and untreated water sources is due to the resistance of *Giardia* cyst to chlorine, protracted and intermitted shedding of the cyst by asymptomatic patients, and a low infective dose required for infection (Hlavsa et al., 2021) The prevalence of foodborne outbreaks of giardiasis caused by contamination from food handlers, animals, or irrigation practices is significantly low compared to waterborne outbreaks (Amahmid et al., 1999; Budu-Amoako et al., 2011).

An epidemiologic study of US giardiasis cases from 1995-2016 found a significant decline in giardiasis in the United States. However, Northeast regions recorded higher rates of transmission. Significantly higher rates of illness were found in males even though the distribution of infection was relatively equal in males and females. Consistent with current literature, children aged 0-4 recorded higher disease rates than other age groups (Coffey et al., 2021). The Centers for Disease Control and Prevention estimates about 1.2 million cases of giardiasis in the United States every year. This number may be an underestimate since many cases of giardiasis are undiagnosed or unreported.

Symptoms of Giardiasis

Giardiasis typically has about two weeks of incubation after ingesting the infective cyst. The disease is usually self-limiting and resolves itself within weeks without treatment. The disease's severity and duration depend on the host's susceptibility, the pathogen's virulence, and the infecting strain's genotype. Although asymptomatic persons account for most giardiasis cases, the symptomatic presentation includes diarrhea, flatulence, bloating, weight loss, abdominal cramping, nausea, malabsorption, foul-smelling stools, steatorrhea, fatigue, anorexia, and chills (Bruce W. Furness et al., 2000). Luminal enzyme deficiencies

and damage to the small intestine are also associated with the disease (Hopkins & Juranek, 1991; Lengerich et al., 1994). Severe and debilitating chronic infections may cause irritable bowel syndrome, chronic fatigue, and post-infectious arthritis (Halliez & Buret, 2013; Painter et al., 2017). A multisite birth-cohort study performed by MAL-ED investigators concluded that early chronic infection with *Giardia*, even without diarrhea, is a risk factor for intestinal permeability and stunted growth (Rogawski et al., 2017).

Diagnosis

Giardia was first seen under the microscope by Antonio van Leeuwenhoek in 1681 when he was examining his stool sample (Dobell, 1920). Currently, several diagnostic stools are available for identifying and detecting the parasite. Among them are ova and parasite microscopy tests, *Giardia*-specific enzyme immunoassay, indirect fluorescent assay, direct fluorescent assay, and molecular assays (Beer et al., 2017). The gold standard for laboratory diagnosis of giardiasis is microscopy with direct fluorescent antibody testing (DFA). This technique is specific and sensitive. It offers an increased probability of detection even when the number of cysts in a stool sample is relatively low (Noel Dunn & Andrew L. Juergens, 2022).

Intermitted shedding of the protozoa makes microscopic detection difficult. For an improved and accurate diagnosis, the CDC recommends multiple stool sample collection (at least three) on different days (Jangra et al., 2020). Specific strain identification requires molecular testing. In the United States, commercial DFA and rapid test kits are available for diagnosis (Noel Dunn & Andrew L. Juergens, 2022).

The CDC recommends giardiasis as a differential diagnosis for all individuals with diarrhea lasting more than three days (Noel Dunn & Andrew L. Juergens, 2022). To

maximize the chances for an economical and quick diagnosis, a thorough patient history that notes risk factors such as recent travel, wilderness exposure, or any situation involving poor fecal-oral hygiene must be taken (Gardner & Hill, 2001).

Treatment of Giardiasis

Treatment of symptomatic giardiasis limits the disease's duration, reduces the risk of post-infection complications, cures symptoms, and reduces the transmission rate (Lalle & Hanevik, 2018). There is no approved human vaccine to provide preventive protection against giardiasis. Effective treatment of giardiasis relies on pharmacotherapy and innate and adaptive immune responses. Commonly administered drugs for treating giardiasis include metronidazole, tinidazole, nitazoxanide, mebendazole, albendazole, and paromomycin. However, metronidazole remains the first line of treatment for giardiasis, with a dose of 250 to 500mg every 8 hours for 7-10 days (Lalle & Hanevik, 2018).

Metronidazole is a bactericidal synthetic drug initially discovered in cultures of Streptomyces spp. (MAEDA et al., 1953). Metronidazole uptake is considered a passive process since there is no described receptor. This prodrug is inactive until it is taken up and enzymatically reduced to highly reactive nitro or nitroso radicals under reducing conditions in anaerobic/microaerophilic organisms (Dingsdag & Hunter, 2018; Lalle & Hanevik, 2018). Reduced metronidazole forms adduct with DNA, free thiols, or protein cysteines (Dingsdag & Hunter, 2018). Adducts induce DNA damage by interfering with DNA helical structure, arresting the cell cycle, and inducing oxidative stress, leading to the parasite's death (Lalle & Hanevik, 2018).

Consistently documented side effects of metronidazole are nausea, headache, vertigo, and a metallic taste in the mouth. Severe side effects, including pancreatitis,

central nervous toxicity, and transient reversible neutropenia, have been associated with using metronidazole (Gardner & Hill, 2001). Metronidazole is known to cause cleft lips in newborns during the first trimester of pregnancy (Gardner & Hill, 2001; Noel Dunn & Andrew L. Juergens, 2022). Despite the high efficacy of metronidazole in treating giardiasis, reports of increasing drug resistance in *Giardia* have been found (Lalle & Hanevik, 2018).

Prevention and Control

Since *Giardia* requires a very low infective dose to establish disease and has a high transmission rate, proactive measures are needed to limit the spread of *Giardia* germs. The following recommended good hygiene practices from the CDC may limit the spread of the disease: hand washing with soap and water, hand washing after every diaper change, avoiding swimming if experiencing diarrhea, especially for children in diapers, boiling untreated water for a minute before drinking, and avoiding eating uncooked foods when traveling in disease-endemic areas (Bruce W. Furness et al., 2000). Iodine should be used for disinfection since the *Giardia* cyst is resistant to chlorination. Commercial filters that comply with the National Safety Foundation (NSF) standard 53 or NSF standard 58 are available for oocyst or cyst reduction (Noel Dunn & Andrew L. Juergens, 2022).

Translation Initiation in Prokaryotes

Protein synthesis is a conserved process in biological systems where the coding sequence of mRNA is translated into an amino-acid sequence of a protein (Rodnina, 2018). Translation comprises four significant phases: initiation, elongation, termination, and ribosome recycling (Rodnina, 2018). The initiation phase is a rate-limiting step in protein synthesis and is highly variable among all three kingdoms. In prokaryotes, initiation may

proceed in the Shine-Dalgarno mechanism or a leaderless initiation pathway (Shine & Dalgarno, 1974; Zheng et al., 2011). Shine-Dalgarno-led initiation comprises a small motif called the Shine Dalgarno (SD) sequence, which is the ribosomal binding site in the 5'-untranslated region (UTR) on mRNA. This sequence binds to the 3' end of the the16S rRNA and recruits the ribosome to the messenger RNA (Shine & Dalgarno, 1974). The leaderless initiation pathway proceeds in a different mechanism. The ribosome is recruited directly to the start codon on the mRNA. Here, the mRNA lacks an upstream signal and a 5'UTR, which generally contribute to ribosome binding and translation efficiency (Zheng et al., 2011).

Initiation

The Shine-Dalgarno initiation pathway is a well-studied process in prokaryotes. The mRNA comprises an extended 5'UTR with the SD sequence about 8-10 bases upstream of the start codon. The SD sequence interacts with a complementary anti-SD sequence in the 16S ribosomal RNA and recruits the 30S small ribosomal subunit to the ribosomal binding site (Nakagawa et al., 2010; Shine & Dalgarno, 1974). Initiation factors 1,2 and 3(IF1, IF2, and IF3) promote the kinetics and fidelity of translation initiation. The binding of initiation factor 1 on the ribosome ultimately defines the A site of the ribosome. IF1 also enhances the activities of IF2 and IF3. IF2 is a GTPase-activating protein. It is the largest prokaryotic initiation factor. The binding of IF2 on the ribosome partially defines the A site of the ribosome. IF2 interacts with IF3. IF2 binds to the initiator tRNA (fMet-tRNAi) and recruits it to the ribosome. IF3 binds at the E site on the 30S small ribosomal subunit. It inhibits the assembly of the 70S large ribosomal unit by interfering with the 50S subunit association. IF3 helps with the initiator fMet-tRNA selection over the

elongator aminoacyl-tRNAs (Milon et al., 2008; Rodnina, 2018). The recruited mRNA aligns with the AUG start codon and forms the 30S initiation complex. IF3 induces a conformational change in the initiation complex. Subsequently, IF3 dissociates to a non-canonical site on the 50S subunit, which rejoins with the 30S initiation complex. IF2 mediates the docking of the 50S subunit, which triggers the hydrolyzes of GTP into GDP. GTP hydrolyzes cause a rotational change in the complex, allowing the 50S and 30S subunits to lock into a stable 70S Preinitiation complex (PIC). IF2-GDP and IF1 dissociate from the complex, which transitions fMet-tRNA in the P site and the formation of the elongation-competent 70S initiation complex (Gualerzi & Pon, 2015; Milón et al., 2012).

Control and Regulation of Translation Initiation

Base-paired structures can regulate initiation within the mRNA. This regulatory mechanism works by blocking or exposing the ribosomal binding site. Secondary structures on the mRNA, small trans-acting RNA's, mRNA binding proteins, and regulatory proteins may induce refolding of the mRNA that alternatively turns on or off the translation process. This mechanism controls translation efficiency by sequestering and exposing the ribosomal binding site. mRNAs with an unfolded RBS have a high translation efficacy (de Smit & van Duin, 1990; Kozak, 2005).

The presence of mRNA-specific repressor proteins controls translation by competing with the ribosome for mRNA binding. The binding of a repressor protein may cause steric hindrance or folding of the mRNA, which ultimately sequesters the ribosomal binding site and blocks the entry of the ribosome (Kozak, 2005). Several mechanisms, including competition between the mRNA and substrates such as tRNA or rRNA, control the binding of the repressor protein.

Archaeal Translation Initiation

The general principle for the translation initiation process in all three domains of life is to allow accurate start codon selection and assembly of an elongation-competent ribosome. However, the molecular mechanism that modulates this process is unique to each domain of life. In Archaeal, the translation initiation process is intriguing since Archaeal shares both prokaryotic and eukaryotic characteristics(Schmitt et al., 2020). Experimental studies on Archaeal translation initiation have elucidated the conserved and domain-specific mechanism of the protein synthesis machinery, which is common to all life domains. Advances made toward understanding the translation initiation process in Archaeal have helped debunk the notion that initiation evolved independently in bacteria and eukaryotes(Benelli & Londei, 2011; Schmitt et al., 2020).

The mRNA plays a crucial part in the initiation mechanism. Most prokaryotic and eukaryotic mRNA has a 5'-UTR which includes determinants for ribosomal binding and recognition. As mentioned, bacterial mRNA may comprise an SD motif that interacts directly with anti-SD motifs in the 16S rRNA (Shine & Dalgarno, 1974). The eukaryotic mRNA lacks the SD motifs. However, it is post-transcriptionally modified with a cap and poly(A) tails that aid in ribosomal recognition and binding. In comparison, most archaeal mRNA lacks a 5'UTR or an SD motif and is not modified after transcription. SD motifs make up a minority of archaeal mRNAs, and about 50% of their mRNA is leaderless, being the most prevalent(French et al., 2007; Schmitt et al., 2020). Complementary binding of the SD motif to an anti-SD sequence facilitates the recruitment

of the small ribosomal subunit. This is followed by the formation of the archaeal initiation complex, which comprises an aIF2-GTP-Met-tRNAi^{Met} ternary complex, aIF1, and aIF1A.

This initiation pathway is often utilized in biscistronic mRNAs. The leaderless mRNAs in archaea may facilitate direct binding of the 30S ribosomal subunit, which is preloaded with initiator tRNA(Benelli & Londei, 2011).

Genomic analyses of the Archaeal transcript have identified homologs of several eukaryotic initiation factors as aIF1, aIF1A, aIF2, and aIF5B. Like in eukaryotes, accurate start codon selection is mediated by aIF1, aIF1A, and aIF2, all in complex with the small ribosomal subunit, methionyl initiator tRNA, and the mRNA. The final steps of the initiation mechanism leading to the formation of an elongation-competent ribosome are regulated by aIF1A and aIF5B(Schmitt et al., 2020).

Eukaryotic Translation Initiation

The initiation process in eukaryotes consists of at least 12 eukaryotic initiation factors(eIF), initiator methionyl-tRNA, and the ribosome that performs an interconnected network of reactions to reconstitute the 80S ribosome with the initiator tRNA placed over the start codon of the mRNA (Jackson et al., 2010). Two pathways initiate translation in eukaryotes. These are cap-dependent and cap-independent initiation. Most eukaryotes undergo the cap-dependent initiation pathway (Pestova & Hellen, 2021). Cap-dependent initiation (Figure 3) begins with the formation of the 43S preinitiation complex (PIC), which comprises a ternary complex consisting of eIF2-GTP and methionyl-tRNA bound to the 40S ribosomal subunit. The eIFs1, 1A, 5, and eIF3 facilitate the formation of the 43S PIC (Hinnebusch & Lorsch, 2012). eIFs1, 1A, and 3 binding to the 40S subunit also induce an open scanning competent conformation (Aitken & Lorsch, 2012). eIF4F complex binds to the 5'end of the mRNA marked by 7-methylguanosine cap and interacts with host factors, including eIF3 and poly(A)-binding protein (PABP) to recruit the 43S PIC to the

mRNA. The eIF4F complex consists of eIF4E, a cap-binding protein, eIF4A, an RNA helicase, and eIF4G, a scaffolding protein that contains the binding domains for PABP, eIF4E, and eIF3(in mammals) (Aitken & Lorsch, 2012). The 43S PIC becomes the 48S initiation complex when loaded onto the 5'end of the mRNA (Querido et al., 2020). The 48S initiation complex subsequently scans the 5' untranslated region of the mRNA for the AUG codon. Start codon recognition causes an arrest of the scanning PIC and the ejection of eIF1. The eIF1 release triggers the GTP hydrolysis of eIF2 to its GDP state facilitated by eIF5, a GTPase-activating protein. Subsequently, the PIC moves into a closed stable conformation with the dissociation of eIF2-GDP and eIF5. The release of eIF2-GDP and several host initiation factors allows the binding of the large 60S subunit to the 40S, which reconstitutes the 80s initiation complex. The newly formed 80s initiation complex is facilitated by eIF5B and is ready to commence elongation (Aitken & Lorsch, 2012; Hinnebusch & Lorsch, 2012).

Figure 3

Diagrammatic Representation of the Eukaryotic Initiation Mechanism

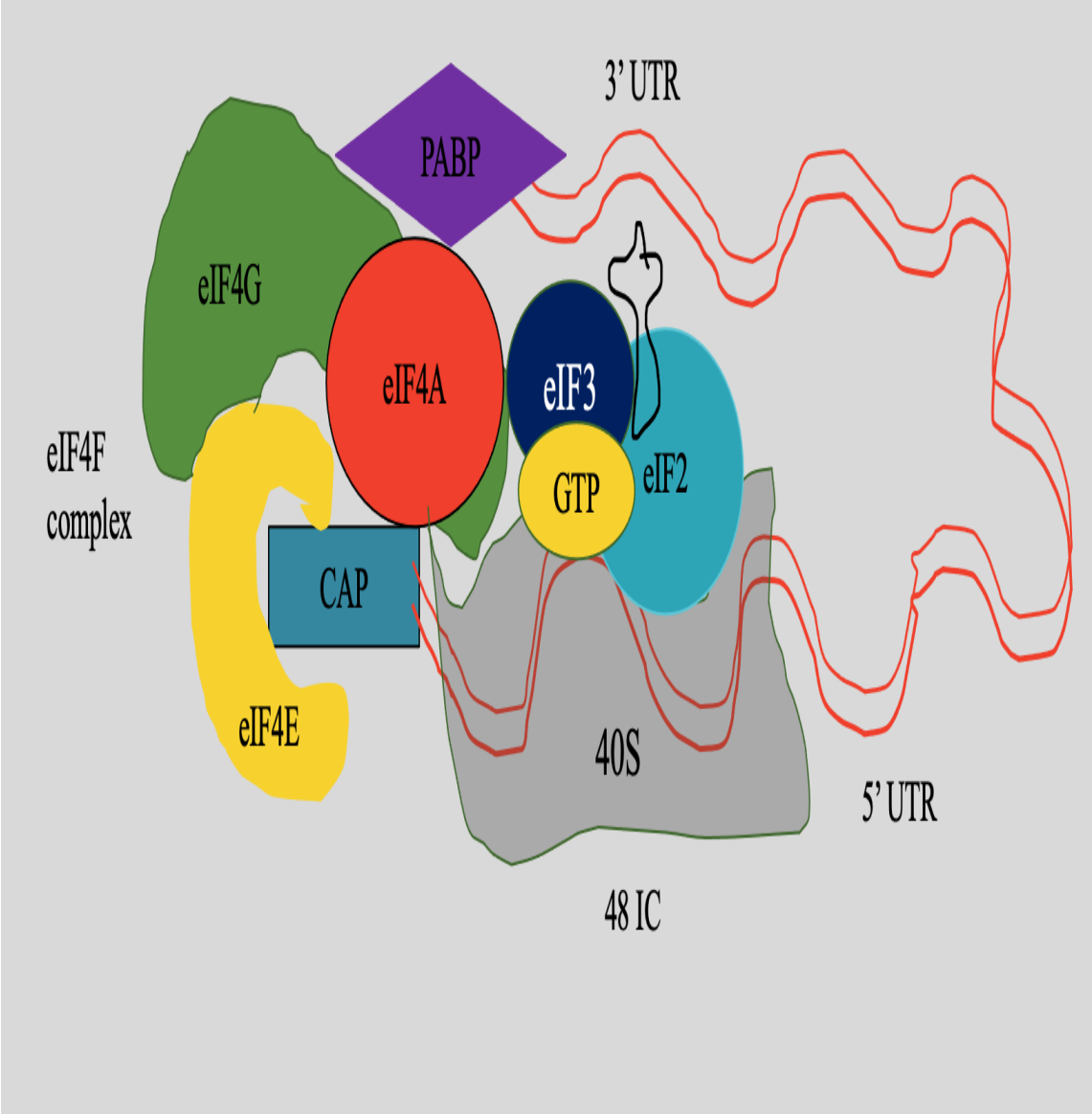

Note. eIF4F complex comprising of eIF4E, eIF4G, and eIF4A is bound to the capped mRNA. Contacts between eIF4G and eIF3 recruit the preinitiation complex, which consists of eIF2-GTP, initiator tRNA, eIF3, and the 40S subunit onto the 5' end of the mRNA.

Regulation of Eukaryotic Translation Initiation

The initiation process is the most regulated phase of the protein synthesis machinery. Regulation of this phase may be mediated by the various eukaryotic initiation factors or the ribosomes, hence universal to all cap-dependent initiation. It may be selective to specific mRNAs using specific RNA-binding proteins (Jackson et al., 2010). eIF2-GTP must load the Met-tRNAi to the 40S subunit. The methionine component on the initiator tRNA has a high affinity for eIF2-GTP than for eIF2-GDP. This high affinity, coupled with the A1:U72 base pair in the acceptor stem of the initiator tRNA, helps select the Met-tRNAi over elongator tRNAs (Hinnebusch & Lorsch, 2012). This specificity in selection is a regulatory role that allows eIF2 to recruit only tRNAi onto the preinitiation complex (Hinnebusch & Lorsch, 2012).

The recruitment of the 43S PIC to the 5' end of the mRNA is a crucial step in the initiation process. The eIF4F complex, which consists of eIF4E, eIF4A, and eIF4G, mediates this step. The eIF4F complex is involved in a series of binding interactions where eIF4E first binds to the m7GpppN cap structure, followed by eIF4G, which recruits eIF4A to the 5'UTR. The eIF4A unwinds secondary structures on the mRNA, allowing eIF4G's interaction with eIF3 to recruit the 43S PIC onto the mRNA. The eIF4F complex assembly is regulated by eIF4E-binding protein(4E-BPs) (Hinnebusch & Lorsch, 2012; Igreja et al., 2014). The 4E-BPs bind to eIF4E and sterically prevent eIF4G from interacting with eIF4E. This steric hindrance causes the inhibition of translation initiation (Igreja et al., 2014).

Cap-independent Translation Initiation

Cap-independent initiation is an alternate pathway that initiates protein synthesis in stressed conditions, viral infections, and mRNAs lacking the prominent m7GpppN cap structure (Spriggs et al., 2010; Yang & Wang, 2019). This initiation pathway utilizes the internal ribosome entry site (IRES) to recruit the ribosome to an internal site of the mRNA and bypass the need for 5'UTR scanning (Pestova & Hellen, 2021). Viral RNAs predominantly contain IRES. However, some cellular mRNA may contain IRES. IRES from different viral families show diversity in sequence and size but have similar secondary structures and initiation mechanisms (Pestova & Hellen, 2021; Yang & Wang, 2019). Various IRES-transacting factors (ITAFs) facilitate initiation via the IRES-dependent mechanism. There are four groups of viral IRES based on their ability to recruit the ribosomal subunit and the level of assistance they require from initiation factors and ITAFS. Compactly folded IRES RNA structures rely less on initiation factors and ITAFS and can interact directly with the 40S ribosome (Johnson et al., 2017).

Giardia Translation Initiation

Giardia is a primitive eukaryotic organism (R. D. Adam, 2021). Debates about its evolutionary history ended with the identification of complete ValRs sequences, elongation factor 1 alpha, and elongation factor 2(Hashimoto et al., 1998). Analysis of the *Giardia* genome shows both prokaryotic and eukaryotic features. These findings suggest that *Giardia* was among the first organisms to branch off in the evolutionary history of eukaryotes (R. D. Adam et al., 2013).

First, the genome complexity of *Giardia* is about $1.2X10^7$bp, with a recorded GC content of 46%. There are no introns in the completely sequenced genome, which contradicts the eukaryotic genome (R. D. Adam, 2021; R. D. Adam et al., 2013). Analysis of the gene transcript revealed various variations in the length of the 5'UTR. The beta-tubulin gene has six nucleotides, whereas other transcripts have a 5'UTR length of 0-14 nucleotides. Experiments aimed at detecting RNA capping showed that most polyadenylated *Giardia* RNAs do not have a cap. From these experiments, 5' phosphorylation did not affect the 5'UTR. Tobacco acid pyrophosphatase showed no decapping effect, and the 5'UTR was susceptible to T4 RNA ligase (R. D. Adam et al., 2013; De-Chao et al., 1998).

Again, a consensus sequence in the coding region of the mRNA with 8 to 13 nucleotides in length has been considered a potential Shine Dalgarno sequence in *Giardia*. This sequence increased translation efficiency in a transfection assay by complementary binding to a 15-base sequence in the rRNA (De-Chao et al., 1998). *Giardia* also has a very short 3'UTR of 10-30 nucleotides (R. D. Adam et al., 2013). The above evidence suggests that *Giardia* may use a straightforward prokaryotic initiation mechanism that does not rely on scanning.

The encystation-induced glucosamine-6-phosphate isomerase B gene has a capped 5'UTR and 146 nucleotide length (Knodler et al., 1999). An encystation gene with a longer 3'UTR and two polyadenylation sites has been determined (Que et al., 1996). *Giardia* may therefore employ a non-canonical eukaryotic initiation mechanism with eIF4F complex bound to the capped mRNA via eIF4E and the subsequent recruitment of the ribosome

through interactions with eIF4G and IF3 following the unwinding of secondary structures on the mRNA by eIF4A.

Homology studies of the parasite's genome have identified homologs for several eukaryotic initiation factors. Identified homologs for the eIF4F complex are eIF4E and eIF4A, as GleIF4E2 and GleIF4A, respectively. Homolog for eIF4G, the scaffolding protein, was not found in *Giardia* (Li & Wang, 2005b). The absence of GleIF4G raises the question of how the preinitiation complex is recruited to the mRNA (Adedoja et al., 2020b). *Giardia* also inherits several eukaryotic initiation factors, including eIF2, six subunits of eIF3, eIF1, eIF1A, eIF5, and eIF5B (Li & Wang, 2004).

Several biochemical and biophysical studies have been performed to solve the puzzled initiation mechanism in *Giardia*. GeIF4E2 has been determined to be a cap-binding protein in experimental research employing m7GTP-Sepharose affinity column chromatography. GleIF4E2 was essential in translation since knockout experiments significantly declined cell growth (Li & Wang, 2005). Recent yeast-two hybrid assay studies detected a protein-protein interaction between GleIF4E2 and GleIF2β (Adedoja et al., 2020b). Inhibition of GleIF4A with Patemine A showed a significant correlation with cell death. This implies that GleIF4A may play an essential function in translation. However, the functional role of GleIF4A is unknown since the relatively short 5'UTRs in *Giardia* are unlikely to form secondary structures (Adedoja et al., 2020).

Studies performed by (Adedoja et al., 2020) proposed that the identified eIF4F homologs in *Giardia* may be sufficient in recruiting the PIC through protein-protein interactions with other factors of the assembled preinitiation complex. Cryo-EM of yeast PICs has shown that eIF2β is close to the mRNA entry channel, and its helix-turn-helix

domain interacts with eIF1, eIF5, and eIF2γ (Anil Thakur et al., 2019). A possible mechanism for recruiting the mRNA onto the entry channel of the ribosome might involve interactions between cap-bound GleIF4E2 with GleIF2β.

Presumably, the mechanistic overview of *Giardia* translation may proceed in a straightforward mechanism with a preassembled initiation complex comprising GleIF1, GleIF5, GleIF2β, and the 40S ribosome. The complex association between GleIF1, GleIF5, and GleIF2β may regulate translation fidelity by promoting an open conformation of the PIC and ensuring accurate start codon recognition. In a swift sequence of reactions, GleIF4E2's interaction with GleIF2β recruits the PIC onto the AUG start codon and destabilizes the PIC into a closed conformation by triggering a dissociation or rearrangement of the GleIF1/GleIF2β complex. The conformational change caused by GleIF2β signals GleIF5 to induce GDP conversion via gated phosphate release. The GTP hydrolysis triggers the release of GleIF1, and several *Giardia* initiations factors, including GleIF2-GDP allowing the assembly of the large ribosomal subunit.

Proving this hypothesis will require using the GST-pull-down assay to characterize the protein-protein interaction between GleIF4E2 with GleIF2β and other host initiation factors.

Protein-Protein Interaction (PPI)

Proteins hardly function in isolation. The functions of proteins are expressed through complex multiprotein associations (Rao et al., 2014). These complex interactions of proteins are responsible for signaling pathways, enzymatic reactions, and structural component assembly (Delahunty & Yates, 2019). Protein-protein interactions also form

the bedrock of biological processes, including DNA replication, transcription, translation, cellular organization, etc. (Rao et al., 2014). There are several types of protein-protein interactions. PPIs may include enzyme-substrate interactions where enzymes bind to their respective substrates to induce a chemical reaction. PPIs can be classified as homo- and hetero-oligomeric complexes, non-obligate and obligate complexes, and transient and permanent complexes. Homo-and hetero-oligomeric interactions occur between proteins with non-identical or identical interacting chains. Obligate complexes are unstable in isolation and become functionally stable only when in a complex association, whereas non-obligate complexes can exist independently. Transient and permanent interactions are distinguished based on the persistence of interaction. Weak protein-protein interactions reflect transient associations, as seen in signaling pathways, while strong and stable associations are permanent interactions (Nooren & Thornton, 2003; Zhang, 2009).

The rapid rise in antimicrobial resistance has highlighted the significance of identifying new therapeutic targets. Pathway-centric therapeutic targets provide a promising solution for combating drug resistance (Ruffner et al., 2007). In translation initiation, the sequential physical interaction of proteins provides an extrinsic function that can be studied to offer pathway-centric novel therapeutic interventions. Characterizing protein-protein interaction is also essential to elucidate an organism's biochemistry. Identifying interacting protein partners can be used to infer the function of a protein within the cell (Rao et al., 2014).

There are several experimental techniques used to detect protein-protein interaction. Notable among them are the Yeast two-hybrid (Y2H) method and affinity purification approach (Rao et al., 2014). Experimental approaches to detect and validate

PPIs are typically designed using In-vivo techniques followed by in-vitro and in-silico confirmatory assays (Delahunty & Yates, 2019; Rao et al., 2014). This experimental design allows for the detection of PPIs in the living organism, validation in a controlled environment outside the cell, and finally, with a computer structure-based approach (Rao et al., 2014).

Yeast Two-Hybrid Assay

Fields and Song first developed the Yeast two-hybrid system (Figure 4). This experimental technique is based on the modular properties of the eukaryotic Gal4 transcription factor (Fields & Song, 1989). Gal4 is a modular protein in yeast that binds to the upstream activation domain (UAS) and activates transcription in the presence of galactose. The functional property of gal4 is distributed across its two domains. The N-terminal domain, also known as the DNA binding domain, binds to the UAS. The C-terminal domain (transcriptional activation domain) activates transcription in the presence of galactose (Keegan et al., 1986). When the two fragments are separated, the N-terminal fragment maintains its ability to bind to DNA. However, it cannot activate transcription in the presence of galactose. This function depends on the presence of the C-terminal fragment. When both fragments are in proximity, they form non-covalent contacts and reconstitute a fully functional Gal4 protein (Keegan et al., 1986). Based on this, a construct of two proteins (X and Y) can be fused to the DNA binding domain and the activation domain of Gal4. If proteins X and Y interact and bring the two fragments into proximity, a fully functional Gal4 is reconstituted, which leads to the expression of a reporter gene(Fields & Song, 1989).

Figure 4

Schematic Representation of a Classical Yeast Two-Hybrid System

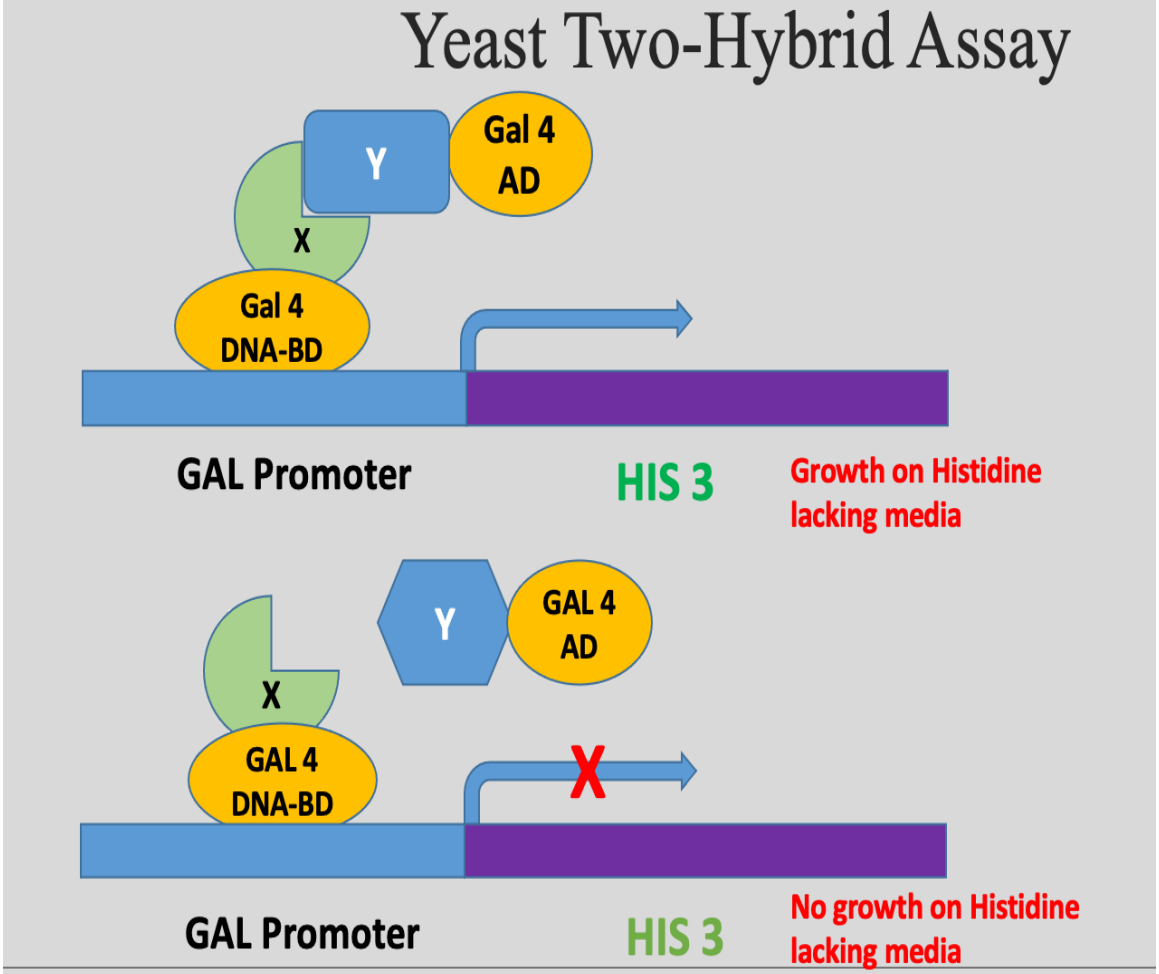

Note. The DNA binding domain and activation domain are functionally and structurally independent. In the first diagram, the physical interaction between protein X and Y brings the DNA-binding domain and activation domain in close proximity to reconstitute a functional Gal 4 transcription factor which leads to the expression of a reporter gene. In the absence of protein-protein interaction between X and Y, the activation domain is unable to localize to the reporter gene to drive gene expression.

GST Pull-Down Affinity Chromatography Assay

Glutathione S-transferase (GST) is a 26 KDA protein. It is an enzyme that occurs naturally in eukaryotes (Smith & Johnson, 1988). GST binds with high affinity to glutathione sepharose matrix through an enzyme-substrate relationship. The robust but reversible binding interaction between GST and glutathione Sepharose matrix allows GST to be utilized as an affinity tag for immobilizing and detecting binding protein partners. A complex association between the GST-fusion protein and an interacting protein can be eluted with reduced glutathione in a non-denaturing buffer (Kim & Hakoshima, 2019; Walls & Loughran, 2011). The GST moiety does not block the accessibility of the fusion protein to its interacting partner since an extended linker region separates GST and the fused protein into individual domains (Vikis & Guan, 2004). The GST-pull-down assay has been highly utilized as a confirmatory and screening tool in proteomic studies (Walls & Loughran, 2011). Successful applications include using GST-pull down assay to characterize P53-binding proteins involved in positive and negative regulation of tumor suppression (Keller et al., 2003).

Since GleIF4E2 was found to interact with GleIF2β in yeast two-hybrid studies, and since GleIF4E2 binds to the m^7GTP Cap analog**,** the observed yeast two-hybrid interaction may be crucial in translation initiation. GleIF4E2 and GleIF2β are likely to interact with other *Giardia* initiation factors to form complexes that recruit the PIC onto the 5' end of the mRNA. The yeast two-hybrid system cannot detect such complex protein-protein interactions. The GST pull-down assay (Figure 5) will be used to map binary and complex protein-protein interaction between GleIF4E2 and GleIF2β and other *Giardia* initiation factors.

Figure 5

Schematic Cartoon of a Classical GST-Pull-Down Assay

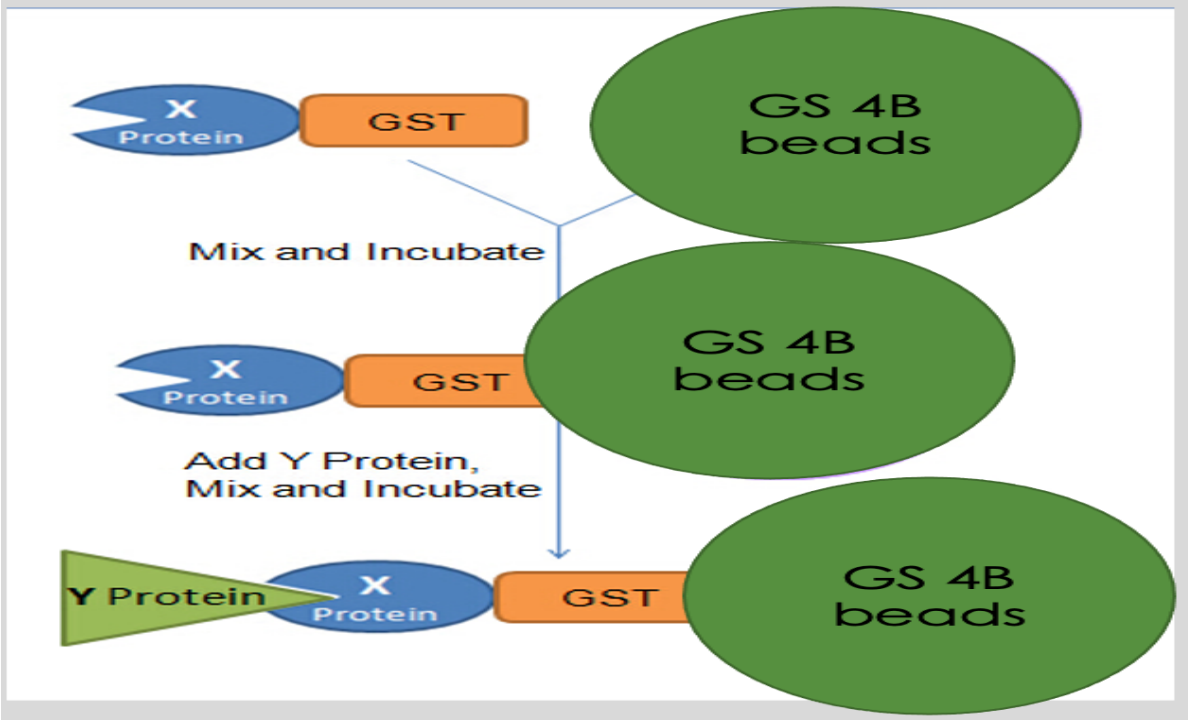

Note. Protein X is expressed and purified as a GST-fusion protein and attached to glutathione sepharose (GS) beads. Protein Y is added to the mixture and incubated for about 2 hours. If protein X has an affinity for Y, they form a GST-X-Y complex which can be eluted and observed on a western blot.

CHAPTER II

Materials and Methods

In this study, recombinant Giardia initiation factor proteins expressed in pGEX and pET expression vector systems were produced in different strains of *E. coli*. The protocols for protein purification, affinity chromatography pull-down assays, and immunodetection were determined and optimized for each target protein. The media components, strains of cells, antibiotics, DNA extraction kits, enzymes, plasmids, solutions and buffers, chemicals, and compounds used in this study are listed below.

Strains

The Shuffle T7 Express Chemically Competent *E. Coli* B and BL21 (DE3) cells were purchased from New England Biolabs (Ipswich). BL21 Star (DE3) was purchased from Thermo Fisher Scientific (Carlsbad, CA), and JM109 competent cells were purchased from Promega Corporation (Madison, WI).

Media Components

Culture media composition used for cell cultivation included: dextrose (Carolina Burlington, NC), Luria-Bertani broth, Miller (Fischer Scientific, Geel, Belgium), Difco Agar (Becton Dickinson and Company, Sparks, Maryland), M9 salts, magnesium sulfate (Fischer Scientific, Fairlawn, NJ), calcium chloride (Fischer Scientific, Fairlawn, NJ), and deionized sterile water.

Antibiotics

Ampicillin (Sigma, St. Louis, MO), Kanamycin, Chloramphenicol, and Tetracycline (Fischer Scientific, Fairlawn, NJ), were purchased to maintain selective pressure in cloning.

DNA extraction

DNA extraction kits for this study included: nuclease-free water, QIAprep spin miniprep kit, QIAquick gel extraction kit (Qiagen, Hiden, Germany), and 1kb DNA ladder (New England Biolabs, Ipswich, MA).

Enzymes and Antibodies

Enzymes and antibodies used for restriction digest and immunodetection were purchased from New England Biolabs (Ipswich, MA).

Plasmids

pGEM T-easy vector kit (Promega, Madison, WI), pET-41a (Figure 6), and pGEX-6p-3 (Figure 7) expression vector systems (EMD Milipore, Billerica, MA) were purchased for protein expression.

Figure 6

Schematic Cartoon of the pET-41a Vector

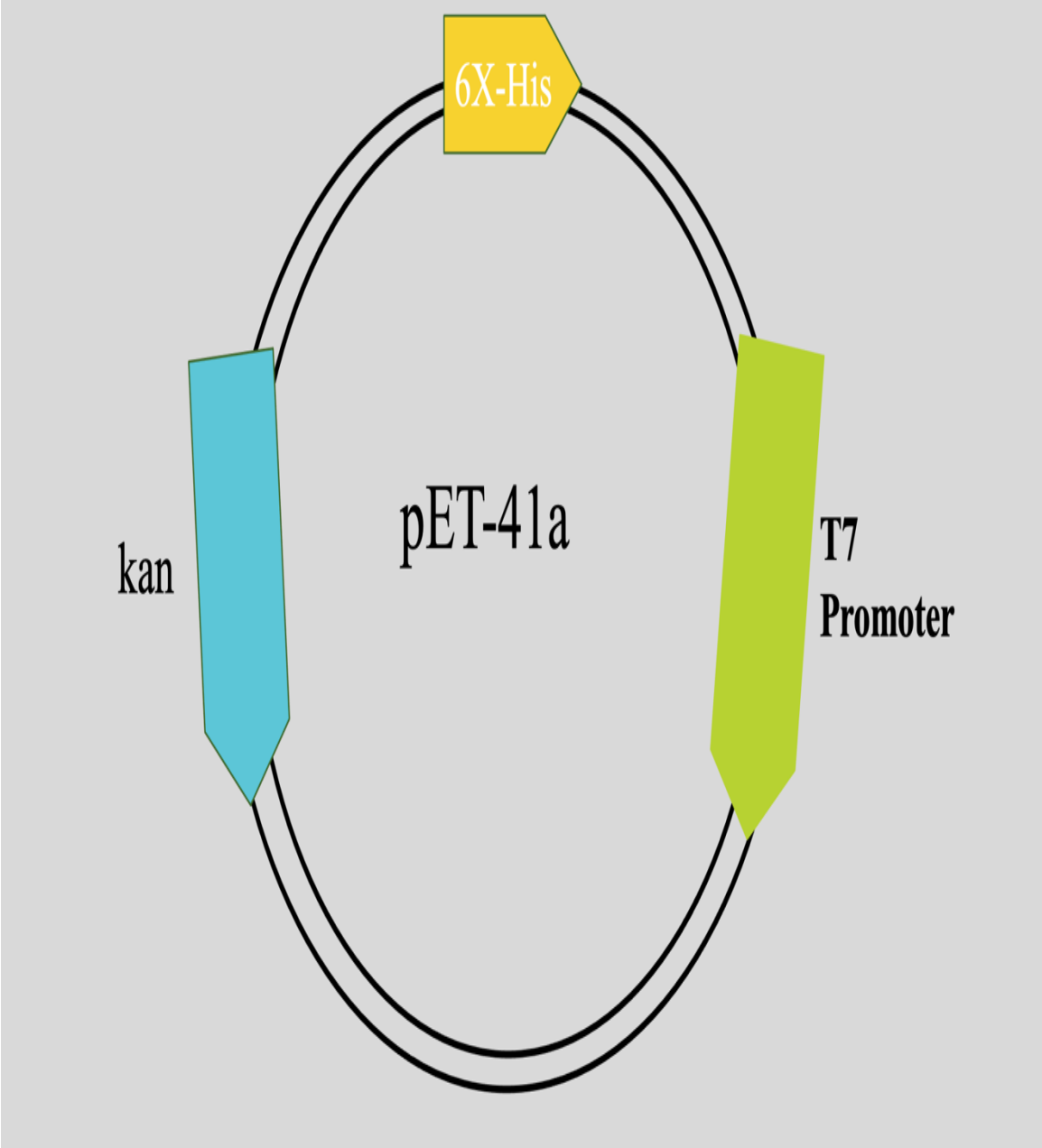

Note. The pET-41a vector was used for expressing hexahistidine-tagged proteins.

Figure 7

Schematic cartoon of the pGEX-6p-3 Vector

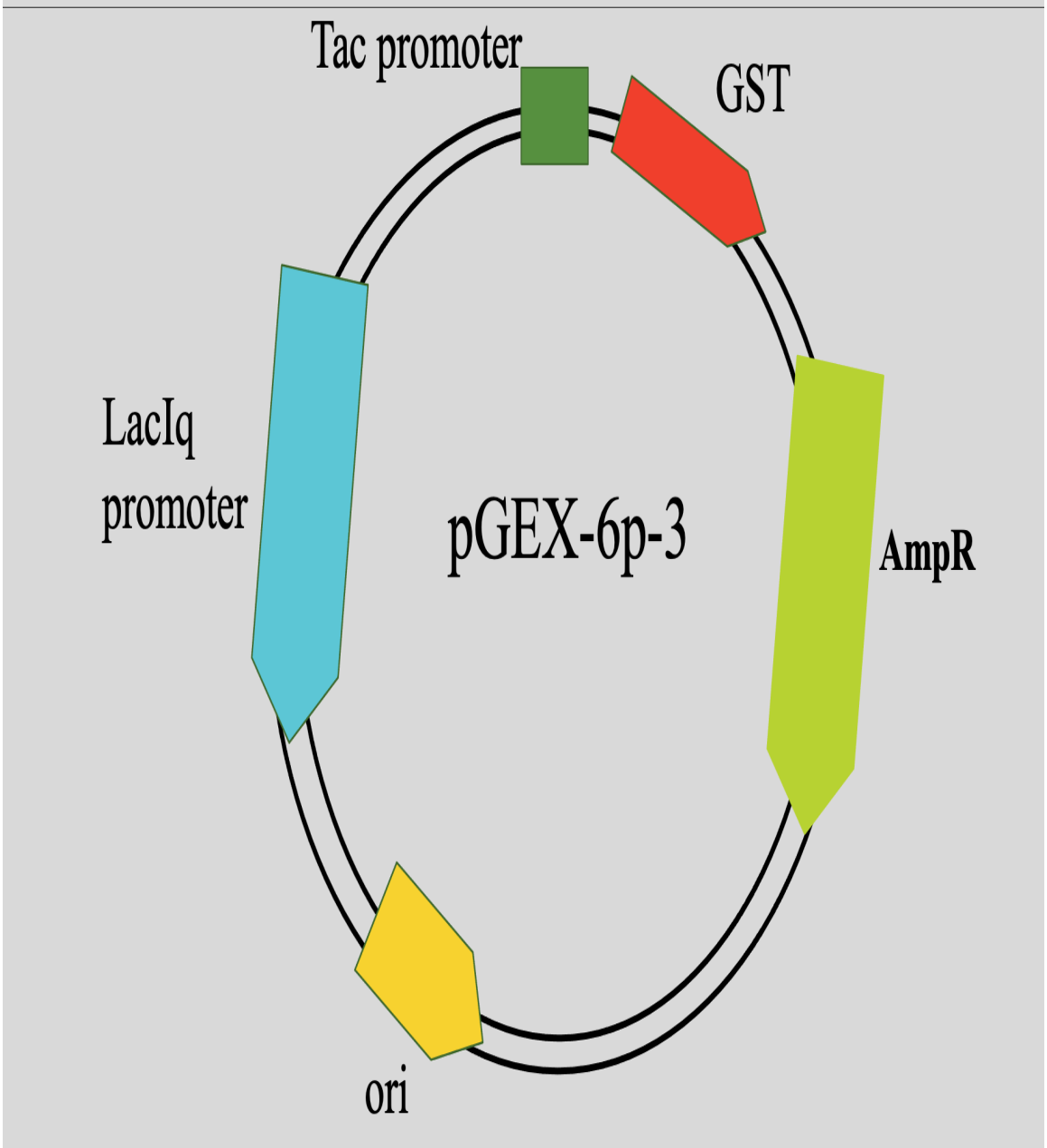

Note. The pGEX-6p-3 bacterial vector was used for expressing GST fusion proteins.

Chemical and Compounds

Materials and compounds used for buffer preparations and experimental assays included: Methanol, Glacial acetic acid, L-Arginine (Sigma-Aldrich, St. Louis Mo), Bovine serum albumin (EMD Millipore Corp. Burlington, MA), Imidazole (Amresco, Solon, Ohio), Hydrochloric acid (Amresco, Solon, Ohio), IPTG (Gold BIO, St. Louis, MO), Triton^{TM} X-100 (Sigma-Aldrich, St. Louis Mo), NaCl (Acros Organics, Israel), Tris-HCl (Thermo Fisher Scientific, Carlsbad, CA), HisPur Cobalt Resin (Thermo Scientific, Rockford, IL), Heparin Sepharose 6 Fast Flow (Cytiva, Sweden), Ni-NTA Superflow (QIAGEN GmbH, Hilden, Germany), Coomassie Brilliant Blue R-250 staining solution (Bio-Rad Laboratories, USA), NP-40 (Thermo Scientific, Switzerland), lysozyme (Thermo Scientific, Rockford, IL), Glutathione sepharose 4B (Cytiva, Sweden), Protease inhibitors (Roche Diagnostics, Mannheim, Germany), and 40% Acrylamide/Bis Solution 37.5:1 (Bio-Rad, China).

Preparation of LB broth (liquid) Medium

LB broth powder (12.5g) was added to 500 mL MiliQ water in a 1L flask. The mixture was stirred with a magnetic stirrer at 110 rpm to dissolve the ingredients completely. Aluminum foil was used to cover the top of the flask, and the flask was placed in an autoclave at 121 °C for 15 minutes on the liquid cycle. After sterilization, the flask was removed from the autoclave and allowed to cool to room temperature. After the medium was cooled, it was transferred into sterile 50 mL tubes and placed in a refrigerator.

Preparation of LB agar plates

Agar plates were prepared by adding 12.5g LB powder and 7.5g of Agar to 500 mL of MiliQ water in a 1L flask. The mixture was stirred to mix and autoclaved at 121 °C for 15 minutes on the liquid cycle. After the cycle, the flask was placed in a 50°C water bath to cool. A 1:1000 dilution of antibiotic was added to the media flask and swirled for about 10 seconds. The media was poured into Petri dishes to cover the bottom of the dish under sterile conditions. The Petri dishes were covered with the lid and stored upside down in an eight °C refrigerator.

Preparation of SDS-PAGE Gel

The glass plates and spacers for the gel casting unit were cleaned with water. The plates and spacers were assembled on an even tabletop surface. The desired percentage of resolving gel was prepared in a final volume of 10 mL and poured into the assembled plates. Water (100µL) was added on both sides of the assembled plates to maintain the gel surface. The gel was allowed to solidify for about 20 minutes at room temperature. The stacking gel solution was prepared in a final volume of 5 mL. The water on the gel was discarded, and the stacking gel was added to the glass plates. A ten-well comb was inserted into the gel and allowed to solidify at room temperature for about 20 minutes.

Cloning of Giardia Initiation Factors into an Expression Vector

Transformation

A pGEM T-easy plasmid containing the inserted gene sequence for Giardia initiation factors was transformed into JM109 competent cells. For high transformation efficiency, 10 µL of the JM109 cells were added into a 1.5 mL Eppendorf tube. To this tube, 2 µL of pGEM T-easy plasmid was added. The cell mixture was left on ice for 20

minutes. After the 20 minutes of ice incubation, the combination was heat shocked at 42 °C for precisely 50 seconds and immediately placed on ice for ten minutes. In sterile conditions, room-temperature LB broth (500 μL) was added to the cell mixture. The tube was incubated for 60 minutes in a 37 °C water bath. After the incubation, the cells were centrifuged at 14000 rpm for 60 seconds. Four hundred microliters of the supernatant LB were decanted. The cell pellet was resuspended in 100 μL of LB and plated on a 100mg/mL ampicillin selection plate. The selection plate was incubated overnight at 37°C.

Plasmid Extraction

A single colony was inoculated from the ampicillin selection plate into a 4mL LB broth containing a 1:1000 dilution of ampicillin. The cell culture was incubated overnight at 37 °C and agitated at 250rpm. The following day, the cells were centrifuged at 4000 rpm for 15 minutes, and the supernatant was decanted. Plasmid DNA was extracted using the QIAspin miniprep kit. Plasmid DNA (40 μL) was eluted and confirmed in a 1% agarose gel electrophoresis, run at 100V for 20 minutes.

Restriction Enzyme Digest and Gel Extraction

The extracted plasmid was digested using the appropriate restriction enzymes. The reaction mixture constituted 2 μL of DNA, 0.5 μL of each enzyme, 1 μL of buffer, and 6 μL of nuclease-free water. The reaction mixture tube was incubated in a 37 °C water bath for two hours. After the incubation, the samples were run in a 1% agarose gel electrophoresis. After the complete gel run, the bottom band was excised, and DNA was extracted using the QIA quick gel extraction kit.

Ligation and Cloning in a Protein Expression Vector

The digested DNA sequences were ligated with pET and pGEX expression vector systems. The ligation reaction was set up with 1 μL of the expression vector, 5 μL of 2X ligation buffer, 4 μL of insert, and 1μL of T4 DNA ligase. The ligation mixture was incubated at 16 °C overnight. The following day, the ligation mixture was transformed into JM109-competent cells. Subsequently, the expression plasmid was extracted from the transformed cells and digested to confirm successful cloning. The plasmid was stored in a four ˚C freezer until ready for downstream processing.

Expression and Purification of GST Fusion Proteins

Transformation

A pGEX expression vector was used for the expression of GST fusion proteins. The pGEX vector has an isopropyl β-D-thiogalactoside (IPTG) inducible tac promoter, which controls gene expression. The pGEX expression vector also contains an internal lacIq gene that binds to the operator region of the tac promoter and represses gene expression until IPTG induction. The pGEX-GleIF4E2 plasmid was transformed into the host *E. coli* BL21 star DE3 by pipetting 10 μL of competent *E. coli* cells into a 1.5 mL transformation tube on ice. Two μl of the plasmid DNA was added to the cells, and the mixture was placed on ice for 30 minutes. The cells and plasmid construct were heat shocked in a 42 ˚C water bath for ten seconds and immediately placed on ice for five minutes. A room-temperature LB broth (500 μL)was added to the mixture under sterile conditions. The tube was placed in a 37 ˚C water bath for 60 minutes. The mixture was then centrifuged at 14000 rpm for one minute, 400 μL of the supernatant LB was pipetted out, and the remaining 100 μL LB and

cell pellet were mixed thoroughly by pipetting up and down. The 100µl mixture was then spread on an ampicillin selection plate and incubated overnight at 37 °C.

Expression

A single colony from the ampicillin selection plate was inoculated in a 4 mL tube with Lb broth and a 1:1000 dilution of ampicillin. The broth was then incubated overnight in a 30 °C shaker at 250 rpm. A 1:100 dilution from the initial 4 mL tube was pipetted into a 50 mL Lb flask with a 1:1000 dilution of ampicillin and incubated in a 30 °C shaker at 250 rpm. The culture was grown until the OD_{600} was 0.6 when measured on a spectrophotometer. The cells were then induced with IPTG to a final concentration of 1 mM for expressing recombinant GleIF42 protein in *E. coli*. Subsequently, the cells were incubated in a 16 °C incubator overnight. The overnight cultured cells were centrifuged in 50 mL and 10 mL falcon tubes at 4000 rpm for 15 minutes. The supernatant was carefully discarded, and the cell pellet was stored in a - 18 °C freezer until ready for downstream processing.

Small-scale analysis of protein expression

Small-scale 10 mL cell pellets were used to determine the solubility or insolubility of the expressed protein of interest. The protocol for protein purification was then generated based on the level of solubility of the expressed protein. The harvested 10 mL cell pellet was first thawed on ice. Bugbuster (1 mL) was added to the cell pellet and mixed thoroughly by pipetting up and down. The mixture was then transferred into a 1.5 mL Eppendorf tube.

A protease inhibitor was added in excess to inhibit protease activity. The cell mixture was centrifuged at 14000 rpm for ten minutes at four °C. The supernatant was

carefully collected into a new 1.5 mL Eppendorf tube without disturbing the cell pellet. The cell pellet was then dissolved in 0.5 mL of water. The supernatant and the dissolved cell pellet were prepared for SDS-PAGE electrophoresis and western blotting. Soluble cytoplasmic recombinant proteins undergo spontaneous folding to maintain their native structure and are detected in the supernatant. Insoluble and misfolded recombinant proteins are seen in the cell pellet.

SDS-PAGE Electrophoresis

The supernatant (30 µL) and resuspended cell pellet were pipetted into 1.5 mL Eppendorf tubes. Then, 10 µL of 4X Laemmli protein sample buffer was added into each tube and boiled for ten minutes to denature proteins for SDS-PAGE analysis. The samples were then centrifuged at 1600 xg for five minutes. Equal volumes of proteins were loaded into the wells of an SDS-PAGE gel along with 5 µL of pre-stained protein standard markers. The gel was run for two hours at 100 Volts.

Western blotting

A PVDF transfer membrane, the size of the gel, was soaked in methanol for 10-15 minutes. The gel was peeled off the glass plate into a box containing 1x transfer buffer and agitated 5-10 times to remove salts and SDS. The gel holder cassette was opened black side down into a casserole dish, and a filter pad was soaked in transfer buffer and placed in the center of the black side. A single filter paper was drowned in the transfer buffer and placed on the filter pad. All bubbles were rolled off the filter paper using a glass tube, and the gel was subsequently placed on top of the filter paper. The glass tube was used to roll out bubbles from the gel, which allowed for the smooth placement of the PVDF membrane on top of the gel, and all bubbles were rolled off the PVDF membrane. A second filter

paper was soaked in the transfer buffer and placed on the PVDF membrane, and all bubbles were again rolled off the filter paper. A second filter pad soaked in transfer buffer was placed on the assembled stack, and all bubbles were finally rolled out using the glass tube. The gel holder cassette was closed and placed in the transfer tank. The tank was filled with 1000 mL of transfer buffer with a sealed ice pack. The transfer was run at 100V for four hours at four ˚C.

Immunodetection

Following western blot transfer, the membrane was placed in a box containing 10 mL of 5% nonfat milk in PBST&T (blocking buffer) on a rocker for overnight blocking. The following day, the blocking buffer was rinsed off two times with PBST&T. GST Tag Monoclonal Antibody (1µl in 10mL) was incubated on the blot for one hour at room temperature. The antibody was then poured into a Falcon tube and saved in the - 18 °C freezer for reuse. The blot was washed thrice with PBST&T for 15 minutes per each wash cycle. A 1 µL in 10 mL Rabbit anti-Mouse IgG-HRP Secondary Antibody was incubated with the blot for an additional hour at room temperature. After the 1-hour incubation, the antibody was collected into a falcon tube and saved in a - 18 °C freezer for future reuse. The blot was washed twice with PBST&T for 15 minutes per wash cycle. Equal volumes of luminal and peroxide (1.5 mL) were added to the blot and agitated for five minutes in a dark room devoid of UV light. The membrane was removed from the box using a pair of forceps and dipped on paper to drain excess fluid. The membrane was placed in a plastic cover and visualized in a Chemidoc imager (Bio-Rad, Hercules, CA).

Large Scale Protein expression

A single colony of the transformed bacterial cells from the ampicillin selection plate was inoculated into a 4 mL LB broth containing a 1:1000 dilution of ampicillin. The culture broth was placed in a 30 °C shaker overnight at 250 rpm. The following day, a 1:100 dilution from the initial 4 mL culture was inoculated into a 250 mL Lb broth with a 1:1000 dilution of ampicillin. The large culture flask was placed in a 30 °C shaker and rocked at 250 rpm. The culture was grown until an OD_{600} of 0.6 was measured. The cells were centrifuged in 50 mL Falcon tubes at 4000 rpm for 15 minutes, and the LB supernatant was decanted under sterile conditions. The cell pellets were resuspended into a 250 mL flask containing minimal media and a 1:1000 dilution of ampicillin. IPTG was added at a final concentration of 1 mM to induce protein expression. The cells were placed in a 16 °C fridge and agitated at 250 rpm for overnight incubation. The following day, the cells were centrifuged at 4000 rpm for 15 minutes, and the LB supernatant was decanted. The cell pellets were then placed on ice for downstream processing.

Affinity Purification of Soluble GST-Fusion Protein

An immobilized glutathione Sepharose 4B resin was used to purify soluble GST fusion proteins. A stock of glutathione beads was prepared with 800μL of glutathione-Sepharose 4B resin pipetted into a column. The glutathione column was washed with five-bed volumes of GST lysis buffer at a flow rate of 1 mL per minute. This was done to eliminate the 20 % ethanol storage solution and attain a 600 μL bed volume of glutathione Sepharose. The cell pellet was washed twice by resuspending it in PBS and excess protease inhibitor. It was centrifuged at 4000 rpm for 15 minutes, and the supernatant was decanted. The washed pellet was again resuspended in a 5 mL GST lysis buffer with a final lysozyme

concentration of 0.1 mg/mL. Excess protease inhibitors were added to prevent proteolytic activities. The cell mixture was left on ice for 20 minutes. The cell mixture was sonicated using a probe-tip sonicator at 50 rpm for 10 seconds and a one-minute pause between each sonication cycle. This was repeated until complete cell lysis was achieved. The cells were kept on ice during sonication to minimize proteolytic activities and minimize frothing. Sonication was done in short intervals to reduce sample heating, and excess protease inhibitors were added post-sonication.

The cell lysate was centrifuged at 18,000 rpm for 20 minutes at four ˚C. The supernatant containing the soluble fusion protein was filtered into the GST Sepharose column through a 0.2 μm filter. Additional protease inhibitors were added in excess to prevent proteolytic activities. The cell suspension was then incubated with the GST Sepharose beads for one hour on a rotator. The flow through was collected into a clean 15 mL Falcon tube for downstream SDS-PAGE analysis. The column was washed with ten-bed volumes of GST lysis buffer for two minutes per wash cycle. The proteins were eluted with reduced glutathione buffer at a flow rate of 1 mL/minute. The eluted fusion proteins were analyzed by SDS-PAGE and were stored at four ˚C.

Dialysis

The dialysis packet was clipped with a floating foam and soaked in a dialysis buffer for about five minutes. The proteins were added to the dialysis packet using a 3 mL syringe. An empty syringe was used to suck bubbles out of the dialysis packet. The dialysis packet was gently lowered into the buffer and stirred at four °C with a stir bar. The pore size of the semipermeable membrane of the dialysis packet allows salts and other molecules to diffuse out of the membrane while the protein molecules are retained. The dialysis buffer

was changed every five hours during the 24-hour incubation period. The following day, the proteins were collected from the dialysis packet into a 1.5 mL Eppendorf tube using a 3 mL syringe. The dialyzed proteins were stored in a - 8 °C freezer until ready for downstream analysis.

Coomassie Blue Staining

After SDS-PAGE electrophoresis, the protein gel was gently transferred into a staining box. The gel was soaked in a freshly prepared Coomassie Blue stain for 30 minutes at room temperature. The stain box was gently agitated during the 30-minute incubation. After the 30-minute stain time, the stain was poured back into a separate bottle and saved for future reuse. The gel was rinsed with water and flooded with the destain buffer, and placed on a gentle rocker for one hour at room temperature.

HIS-Tag Fusion Proteins Purification

Double Transformation

The gene for the protein of interest was cloned into a pET vector. The pET vector utilizes the T7 bacteriophage RNA polymerase gene to promote high-level transcription and protein expression. The bacteriophage RNA polymerase is exclusive to the T7 phage genome, is highly specific to the T7 promoter sequences, and is rarely encountered in other genomes. Thus, the expression of the gene of interest is controlled in an inducible bacterial cell engineered to carry the T7 RNA polymerase. LacUV5 promoter controls the T7 RNA polymerase gene and is induced by adding IPTG to the cell culture. The pET plasmid construct was co-transformed with pG-KJE8 plasmid into *E. coli* BL21 Star (DE3) or SHuffle T7 Express E. coli strain. This was done by adding 15 µL of competent *E. coli* cells into a 1.5 mL Eppendorf tube on ice. Alternatively, 2 µL of pET plasmid and pG-

KJE8 plasmid were added to the cell mixture. The suspension was left on ice for 30 minutes. After 30 minutes of ice incubation, the suspension was heat shocked in a 42 °C water bath for ten seconds and immediately placed on ice for five minutes. LB broth (500 μL) at room temperature was added to the suspension under sterile conditions and placed in a 37 °C water bath for one hour. The cells were centrifuged at 13,000 rpm for one minute, and 400 μL of the supernatant was decanted. The remaining 100 μL LB was used to resuspend the cell pellet and plated on a kanamycin/chloramphenicol selection plate. The Shuffle T7 Express cells allow the formation of disulfide bonds in the cytoplasm. The pG-KJE8 plasmid expresses chaperones dnaK-dnaJ-grpE and groES-groEL (Figure 8). The expression of chaperones enables protein folding and solubility.

Expression of pET/pG-KJE8 plasmids

A single colony from the kanamycin-chloramphenicol selection plate was inoculated in 4 mL LB broth containing 1:1000 dilution of kanamycin and chloramphenicol. The 4 mL culture was incubated overnight in a 30 °C shaker at 250 rpm. The following day, a 1:100 dilution from the initial 4 mL LB broth was inoculated into 250 mL LB broth containing a 1:1000 dilution of kanamycin and chloramphenicol. L-Arabinose was added to the cell culture to a final concentration of 0.15 mg/mL. Subsequently, tetracycline was added to the cell culture to a final concentration of 5 ng/mL. This was done to induce the expression of pG-KJE8 (Figure 8). The cell culture was grown in a 30 °C incubator at 250 rpm until the OD_{600} of 0.6 was measured. The cell culture was centrifuged at 4000 rpm in 50 mL Falcon tubes. The LB supernatant was decanted under sterile conditions, and the cell pellet was resuspended into a 250 mL flask containing minimal media with a 1:1000 dilution of kanamycin and chloramphenicol. Previously

mentioned concentrations of L-arabinose and tetracycline were added. IPTG was added to a final concentration of 1 mM. The cell culture was grown in a 16 °C incubator and agitated at 250 rpm overnight. The cultured cells were centrifuged at 4000 rpm in 50 mL falcon tubes the following day. The supernatant was decanted, and the cell pellet was stored in a - 18 °C freezer until ready for downstream processing.

Figure 8

Schematic Cartoon of the pG-KJE8 Plasmid

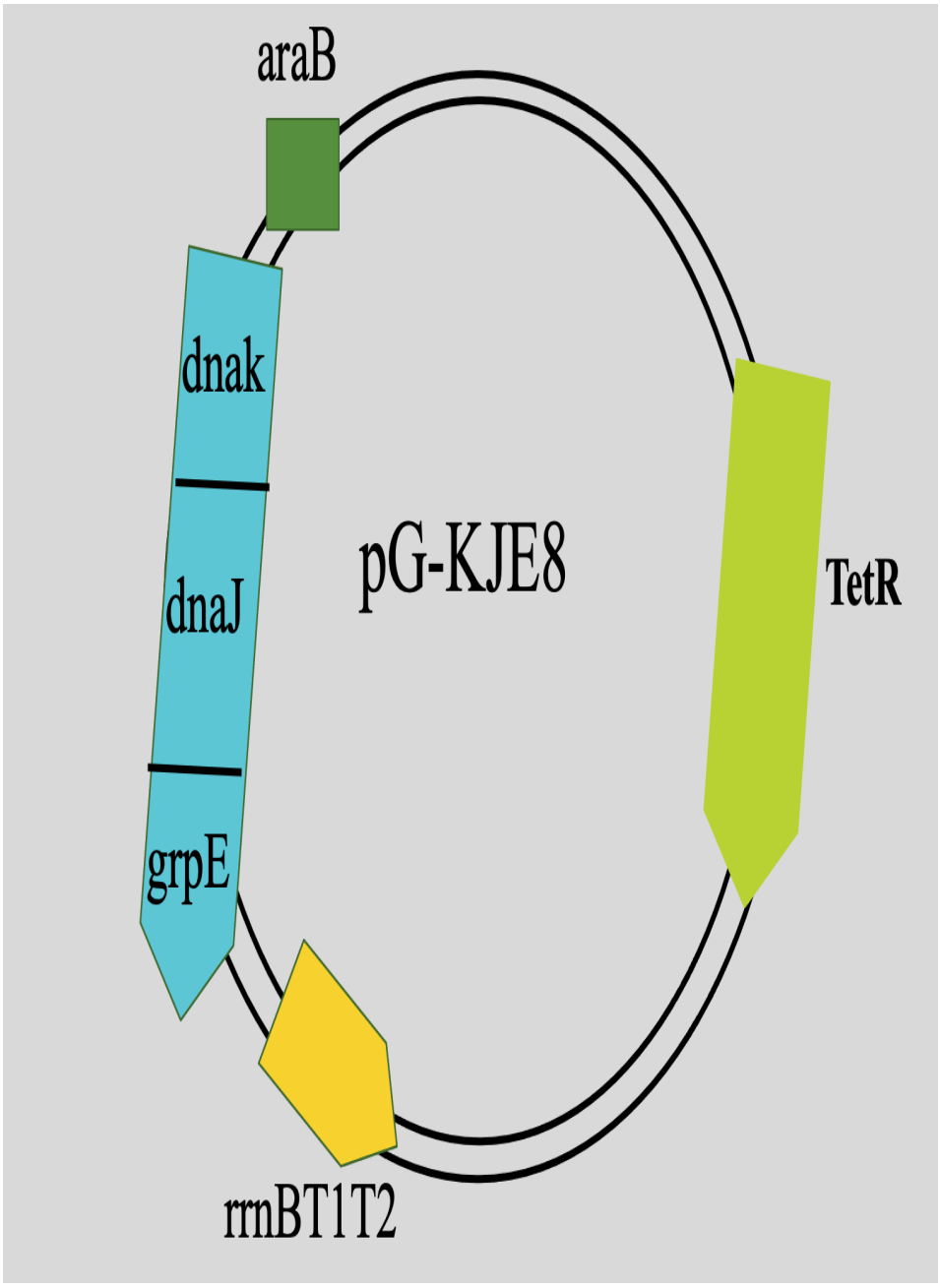

Note. The pG-KJE8 chaperone plasmid was used to induce proper protein folding.

Ni-NTA Affinity Chromatography Purification

Ni-NTA affinity purification of His-tagged fusion proteins is based on the binding affinity of histidine residues for immobilized Nickel ion (Ni^{2+}). Nickle ion is immobilized on a chromatographic matrix by nitrilotriacetic acid (NTA). The interaction between the histidine tag and the metal is captured on the matrix and eluted under native or denaturing conditions. NTA has four metal-chelating sites, providing a stable binding capacity for the metal and preventing Nickel-ion leaching.

The cell pellet was thawed on ice for 15 minutes and resuspended in 5 mL of Ni-NTA lysis buffer for this purification. An excess protease inhibitor was added to the cell suspension to prevent proteolytic activity. The Ni-NTA lysis buffer was prepared with ten mM imidazole to limit the activity of non-specific binding proteins and contaminants. Lysozyme was added to the cell suspension to a final concentration of 0.1 mg/mL. The cell suspension was left on ice for 20 minutes. The cells were sonicated using a probe-tip sonicator at 50 rpm for 10 seconds with one-minute pauses between each sonication cycle. This was repeated until complete cell lysis was achieved. Universal nuclease was added to a final concentration of 5 μg/mL and incubated in a 37 °C water bath for 15 minutes. Excess protease inhibitor was added to the cell suspension to prevent proteolytic activity, and the cell lysate was centrifuged at 18,000 rpm for 20 minutes at 4°C. The supernatant (10 mL) containing the soluble fusion protein was filtered through a 0.2 μm filter into a column containing a 1.25 mL bed volume of washed Ni-NTA. The mixture was placed on a rotator at four °C for 60 minutes. After incubation, the flow through was collected into a Falcon tube for SDS-PAGE analysis. The Ni-NTA column was washed with 5 mL of Ni-NTA wash buffer for five wash cycles. The Ni-NTA wash buffer contains 20 mM

imidazole concentration to prevent non-specific binding proteins and contaminants. A protease inhibitor was added to the wash buffer to prevent proteolytic activity. The purified proteins were eluted with 0.5 mL of Ni-NTA elution buffer and were subjected to secondary purification.

Cobalt Secondary Purification

The cobalt chelating resin was used to co-purify recombinant histidine fusion proteins. The histidine residues have a high affinity and binding specificity for cobalt chelating resin, which allows a single-step purification of the protein of interest. A 1 mL bed volume nickel resin was washed twice with Ni-NTA wash buffer, and the eluted Histidine tagged fusion proteins were incubated with the cobalt resin in a column for one hour on a rotator at four ˚C. A protease inhibitor was added in excess to prevent proteolytic activity. After the incubation, the flow through was collected for SDS-PAGE analysis, and the column was washed with five-bed volumes of Ni-NTA lysis wash buffer. The proteins were eluted with 0.5 mL of Ni-NTA elution buffer, and the eluted proteins were analyzed with SDS-PAGE.

Heparin Sepharose Purification

DNA-binding proteins are a diverse group of proteins functionally involved in replication, the orientation of the DNA, and transcription. They include histones, nucleosomes, replicases, and RNA/DNA polymerase. The ability of DNA-binding proteins to stick non-specifically to proteins can confound the purification of pure proteins. Heparin is a sulfonated glycosaminoglycan that can bind to DNA-binding proteins, serine protease inhibitors, enzymes, and lipoproteins. The interaction of heparin and DNA-binding proteins mimics the polyanionic structure of the nucleic acid and can be utilized as a

secondary purification protocol to clean up or remove DNA-binding proteins. The heparin Sepharose beads were washed with a 150 mM salt buffer and pipetted into a column. The eluted proteins were added to the heparin column. A protease inhibitor was added in excess to prevent proteolytic activity. The suspension was incubated on a rotator at four °C for one hour. After incubation, the flow through was collected into a clean Eppendorf tube. The pure proteins were eluted with 0.5 mL of an increasing salt gradient buffer from 300 mM to 3 M concentration, and the eluted proteins were collected into separate 1.5 mL Eppendorf tubes. SDS-PAGE electrophoresis was used to check the purity of the expressed proteins. Subsequently, the proteins were dialyzed to eliminate the excess salt concentration and stored in a - 4 °C freezer until ready for downstream processing.

GST Pull-Down Assay

Preparation of glutathione Sepharose 4B

GST pull-down assay was used to detect protein-protein interaction *in vitro*. Several binary, complex, and multi-complex interaction sets were tested using the purified GST-fusion proteins and his-tagged fusion proteins. The GST-fusion proteins were labeled as bait proteins, and the his-tagged fusion proteins were labeled prey proteins. The purified recombinant proteins were thawed on ice. The GST Sepharose 4B bottle was gently shaken to resuspend the matrix. The tip of a p1000 pipette was cut off and used to dispense 800 µL of slurry into a 1.5 mL Eppendorf tube. The tube was centrifuged at 800 rpm for one minute at four °C to sediment the matrix and the supernatant was decanted. The Sepharose 4B was washed twice by resuspending it in 400 µL of GST binding buffer and rotated for two minutes. After each wash cycle, the tube was centrifuged at 800 rpm for one minute, and the supernatant was decanted. This was done to remove the 20 % storage ethanol

solution. GST binding buffer (800 μL) was added to the sepharose 4B and thoroughly mixed to make a 50 % slurry.

Binding of GST fusion proteins

Forty microliters of the 50 % glutathione sepharose 4B slurry were pipetted into 1.5 mL Eppendorf tubes, and 800 μL of the GST binding buffer was added to the slurry. The bait GST-fusion protein and protease inhibitor were added to the reaction mixture and incubated on a rotator for one hour at four ˚C, and the tube was then centrifuged at 800 rpm for one minute. The supernatant was carefully decanted using a p200 pipette. Bovine Serum Albumin buffer (800μl of a 5% solution) and a protease inhibitor were added to the sepharose 4B matrix and rotated for one hour at four ˚C. The tube was. Then centrifuged at 800 rpm for one minute, and the supernatant was decanted. The reaction mixture was washed twice with 800 μL of the GST binding buffer by rotating the tube for two minutes on a rotator and allowing the matrix to sediment in a centrifuge at 800 rpm for one minute. The supernatant was carefully decanted.

Pull-down of His-tagged fusion proteins

Purified His-tagged fusion protein was added to the reaction mixture. Subsequently, 800 μL of the GST binding buffer and 40 μL of protease inhibitor were added to the reaction mixture. The reaction mixture was placed on a rotator for two hours at four ˚C. After incubation, the sepharose 4B matrix was washed twice using the GST binding buffer. The tube was centrifuged at 800 rpm for one minute, and the supernatant was carefully decanted. After the two wash cycles, a second, third, or fourth his-tagged fusion protein was added for complex and multi-complex interaction assays. For every added protein, the reaction was incubated on a rotator for two hours at four °C. After this, the tube was

centrifuged at 800 rpm for one minute at four ˚C. The supernatant was carefully decanted without disturbing the sediments. GST elution buffer (30 μL) and 4X Laemmli protein sample buffer (10 μL) were used to elute the proteins and analyzed by Western blotting.

The m^7GTP Cap-binding assay

The m^7GpppN cap structure is a prominent feature of the eukaryotic mRNA that facilitates the binding of the ribosome to the mRNA during initiation. The cap structure has N-7-substituted positively-charged guanosine and a negatively-charged α-phosphate. Electronic interaction between the oppositely charged components maintains the cap in a rigid anti-configuration. This structural feature of the cap is essential for the effective recognition of the ribosome during the initiation of protein synthesis. The cap structure has a high binding affinity and specificity for cap-binding proteins. The ligand-substrate binding specificity of the cap structure can be utilized to purify or pull down cap-binding proteins.

Five hundred microliters of the m^7GTP cap analog linked to sepharose beads were pipetted into a 1.5 mL Eppendorf tube. For accurate pipetting, the tip of the p1000 pipette was cut off. The beads were washed with 500 μL of buffer A by rotating the Eppendorf tube on a rotator for two minutes at four ˚C. After the wash cycle, the tube was centrifuged at 1000 rpm for two minutes at four ˚C, and the supernatant was carefully decanted. A 50 % slurry was made by adding 500 μL of deionized water into the sepharose beads. One hundred microliters of the 50% slurry were pipetted into a clean 1.5 mL Eppendorf tube. GleIF4E2 wildtype and mutant cap-binding proteins (60 μL each) were added individually into Eppendorf tubes containing the sepharose beads. Buffer A (800 μL) and a protease

inhibitor were added to the suspension and incubated on a rotator for four hours at four ˚C. After incubation, the tubes were centrifuged at 1000 rpm for two minutes at four ˚C, and the supernatant was collected for SDS-PAGE analysis. Alternatively, the m^7GTP sepharose beads were washed twice with buffer A. After the last wash cycle, the proteins of interest were eluted with 4X Laemmli protein sample buffer and placed at room temperature for ten minutes. Subsequently, they were analyzed using SDS-PAGE and Western blotting.

CHAPTER III

Results

Validating Protein-Protein Interactions between Cap-Binding Protein GleIF4E2 and the Translation Initiation Factor GleIF2β using GST-Pull-Down Assays:

Studies performed by Adedoja et al. (2020) involved the fusion of cap-binding protein GleIF4E2 to the DNA binding domain (BD) of the GAL4 transcription factor to examine protein-protein interactions (PPIs) with the translation initiation factors of the pre-initiation complex fused to the activation domain (AD) of the GAL transcription factor. In this study, they identified a novel interaction between BD-GleIF4E2 and AD-GleIF2β. Interestingly, the interaction between GleIF4E2 and GleIF2β was not observed when the orientation of the fusion partners was switched. These results suggested that the observed interaction between GleIF42 with GleIF2β is domain-specific, and when GleIF2β is fused to the DNA binding domain, the interacting domain is misfolded or not accessible (Adedoja et al., 2020). Arguably due to this limitation of the yeast two-hybrid system and to increase the accuracy of the reported data set, alternate approaches must be employed to validate the PPIs observed in yeast two-hybrid assays.

In GST pull-down assays, recombinant glutathione S-transferase (GST) fusion proteins expressed and purified from *E. coli* are used as probes to study and validate PPIs *in vitro*. The high-affinity enzyme-substrate relationship between GST and glutathione conjugated resin allows the GST fusion protein (bait protein) to be immobilized on the resin and trap interacting protein partners (hexahistidine-tagged prey proteins) through

specific PPIs. This principle was utilized in testing binary and multi-factor protein interactions in the current study. An internal control consisting of the 26 kDa GST protein alone was tested against the prey proteins of interest to rule out false positive interactions. Western blot analysis was carried out using antibodies raised against the hexahistidine tag to detect the binding of hexahistidine-tagged prey proteins to the GST-fused bait protein. In addition to validating PPIs between GleIF4E2 and GleIF2β, specific amino acid substitutions, L12A, F45A, and F46A, in GleIF4E2 that disrupt its interaction with GleIF2β were also tested.

Initiation factor GleIF2β was expressed and purified as hexahistidine (6his) tagged recombinant protein from *E. coli* (Figure 9, lane 2), whereas the wildtype and mutant (L12A, F45A/F46A, L12A/F45A/F46A) versions of GleIF4E2 were purified as GST-fusion proteins (Figure 9, lanes 3-6). The 26 kDa GST protein alone was also expressed and purified from *E. coli* (Figure 9, lane 1) and was a negative control in GST-pull-down assays. Recombinant GleIF2β-6his strongly interacted with the wildtype GST-GleIF4E2 (Figure 10, lane 2) but not with GST protein alone (Figure 10, lane 1). The lack of interaction between GleIF2β-6his and GST protein alone suggests that PPI observed between GleIF2β and GleIF4E2 is specific. A significantly weak to no interaction was observed between GST-GleIF4E2 single mutant L12A (Figure 10, lane 3) and triple mutant L12A/F45A/F46A (Figure 10, lane 5) with GleIF2β-his compared to the wild type GleIF4E2 (Figure 10, lane 2). GleIF4E2 double mutant F45A/F46A displayed moderate binding to GleIF2β-6his (Figure 10, lane 4).

Figure 9

Coomassie Blue Stained Gel Electrophoresis of Purified Recombinant Proteins

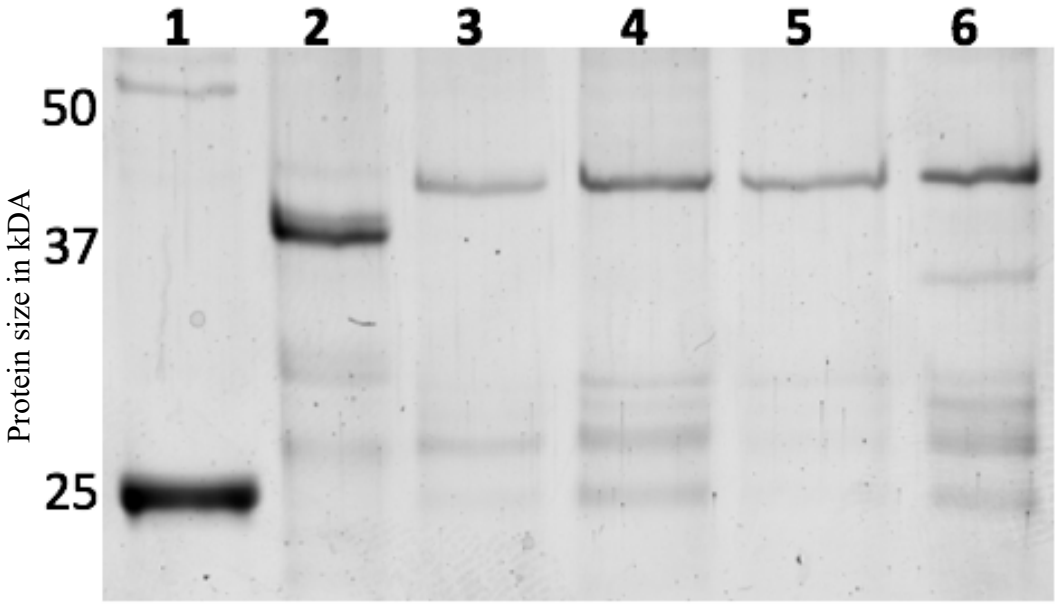

Note. Coomassie blue stained polyacrylamide gel electrophoresis of purified recombinant GST (lane 1), GleIF2β -6his (lane 2), GST-GleIF4E2 wildtype (lane 3), GST-GleIF4E2 L12A (lane 4), GST-GleIF4E2 F45A/F46A (lane 5) and GST-GleIF4E2 L12A/F45A/F46A (lane 6). Protein sizes in kDa are indicated on the left. Individual protein lanes are numbered from one to six.

Figure 10

Western Blot Analysis of PPI between GleIF4E2 WT and Mutants and GleIF2ß-his

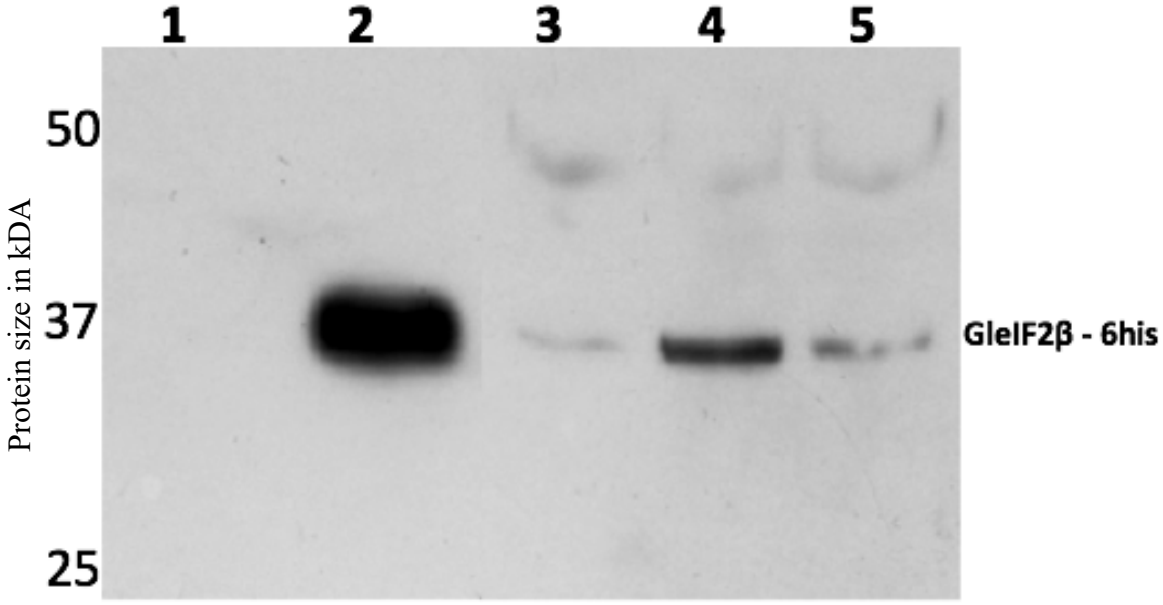

Note. Western blot analysis using anti-6His antibody to detect binding of GleIF2ß-his to GST (negative control; lane 1), GST-GleIF4E2 wild type (lane 2), GST-GleIF4E2 L12A (lane 3), GST-GleIF4E2 F45A/F46A (lane 4) and GST-GleIF4E2 L12A/F45A/F46A (lane 5). Protein sizes in kDa are indicated on the left. Individual protein lanes are numbered from one to five.

To rule out the possibility that the mutations L12A, F45A/F46A, and L12A/F45A/F46A induce changes in the overall conformation of GleIF4E2 and that these changes affect its binding to GleIF2β, homology models of the wildtype and the mutant versions of GleIF4E2 were generated using SWISS Model program (Figure 11). Substitution of amino acid leucine at position 12 to alanine in the β-sheet on the dorsal surface of GleIF4E2 did not alter the overall conformation of the protein (Figure 11, panel B). Similarly, substituting both phenylalanines at positions 45 and 46 (F45, F46) in the α helix located on the dorsal surface of the protein also did not alter the overall conformation of the protein (Figure 11, panel C). Finally, substituting all three amino acids (L12, F45, F46) induced no significant changes in the protein conformation (Figure 11, panel D).

To further confirm that amino acid substitutions do not alter the overall structure of the protein, m7GTP cap binding assays were performed (Figure 12). The rationale for this assay is that if amino acid substitutions induce conformational changes in the protein, these changes may alter the protein's function- the ability to bind m7GTP cap. The GST fusion proteins of the wildtype (Figure 12, lane 2), L12A single mutant (Figure 12, lane 3), F45A/F46A double mutant (Figure 12, lane 4), and L12A/F45A/F46A triple mutant (Figure 12, lane 5) proteins all bound with equal affinity to m7GTP Sepharose. The lack of binding of GST protein alone to the m7GTP Sepharose (Figure 12, lane 1) indicates that the binding of the wildtype and mutant proteins to the m7GTP cap is specific.

These results suggest that the mutations did not alter the structure or the function of the GleIF4E2. Thus, the disruption of its interaction with GleIF2β is not due to overall structural changes.

Figure 11

Homology Models of GleIF4E2 Wildtype and Mutant Proteins

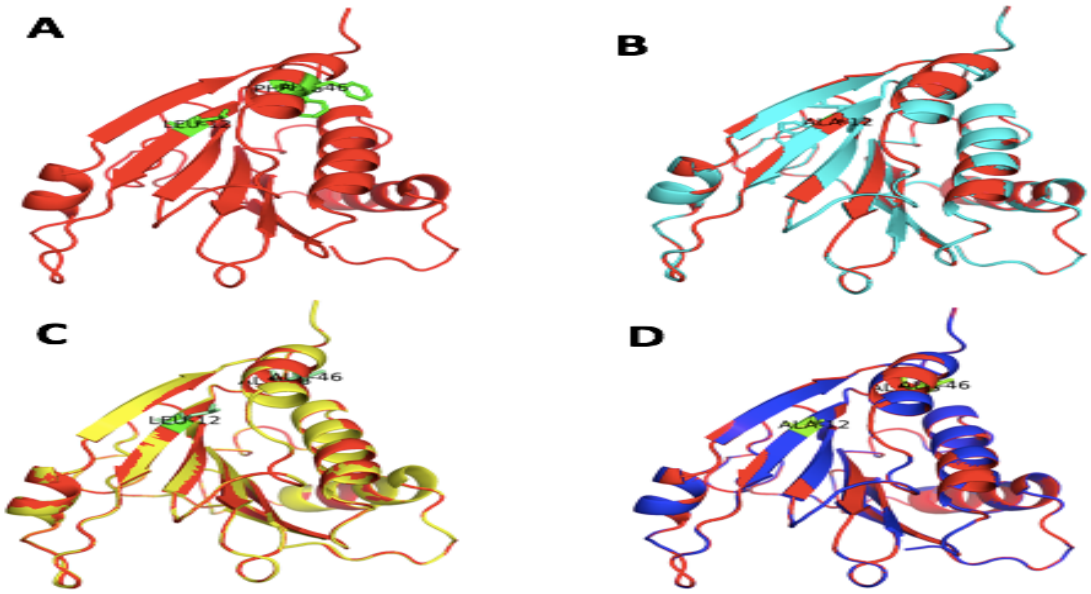

Note. Homology models of GleIF4E2 wildtype (A) using the crystal structure of the human 4EHP-GIGYF1 complex as a template. The homology models of wildtype GleIF4E2 were superimposed onto the homology models of GleIF4E2 L12A mutant (B), GleIF4E2 F45/F46A double mutant (C), and GleIF4E2 L12A/F45A/F46A triple mutant (D).

Figure 12

Western Blot Analysis of the m^{7}GTP Sepharose Assay

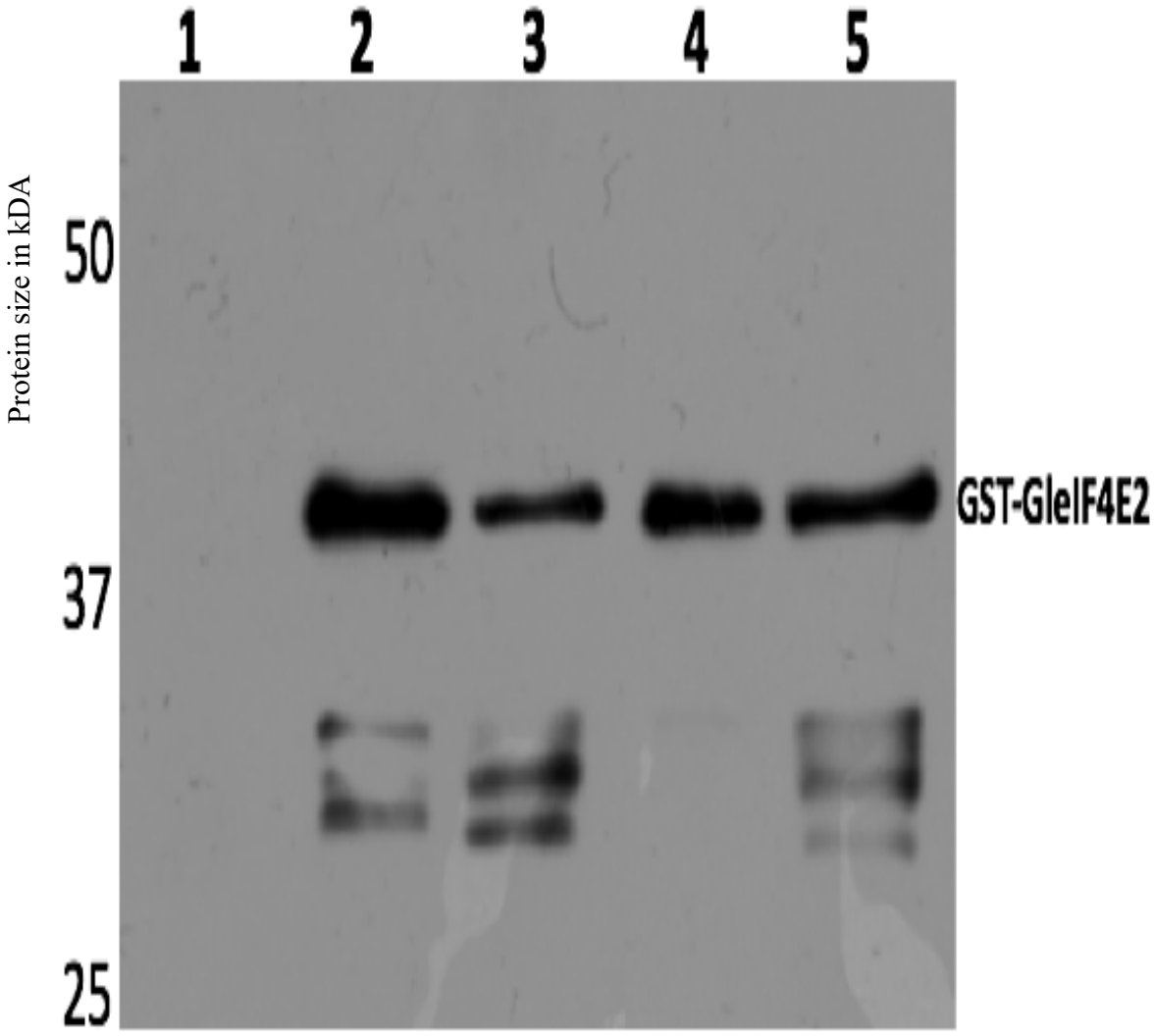

Note. Western blot analysis using an anti-GST antibody to detect binding of GST (negative control; lane 1), GST-GleIF4E2 wild type (lane 2), GST-GleIF4E2 L12A (lane 3), GST-GleIF4E2 F45A/F46A (lane 4), GST-GleIF4E2 L12A/F45A/F46A (lane 5) to m^{7}GTP Sepharose. Sizes of standard protein markers are indicated on the left. Individual protein lanes are numbered from one to five.

GleIF2β Shares an Overlapping Binding Interface with GleIF1, GleIF4E2, and GleIF5:

In higher-order eukaryotes, the eIF2β subunit is known to mediate the interaction of the trimeric eIF2 complex with several components of the pre-initiation complex. In yeasts and mammals, biochemical and genetic approaches have identified PPIs of eIF2ß with eIF1, eIF3 subunit a, and eIF5, which play a key role in accurate start codon recognition during the scanning process (Figure 13A). The eIF2ß subunit has a poorly conserved amino-terminal region and a highly conserved carboxyl-terminal region in yeasts and mammals (Figure 13B). The amino-terminal region of eIF2ß is highly unstructured and contains three stretches of lysine (K1, K2, and K3 boxes) known to mediate binding to eIF1 and eIF5. The structured carboxyl-terminal region facilitates mRNA binding and starts codon recognition via its zinc-finger motif (Figure 13B). In yeasts, mutations in the lysine stretches inhibit cell growth, underscoring the significance of eIF2ß-NTD. In *Giardia*, GleIF2β has poorly conserved lysine and arginine stretches in its unstructured amino-terminal domain (Figure 13B). To determine the role of lysine and arginine stretches of GleIF2β in PPIs with GleIF1, GleIF5, and GleIF4E2 in *Giardia*, they were mutated to alanine residues, and their effect on PPIs was tested in GST-pull down assays. The mutated GleIF2β-NTD lysine/arginine stretches were named KR1, KR2, and KR3 Mut, respectively (Figure 13B). The wildtype (Figure 14A, lane 2) and KR mutants (Figure 14A, lanes 3-5) of GleIF2β were expressed and purified as hexahistidine-tagged fusion proteins from *E. coli*. The GST-fusions of GleIF5 and GleIF1 (Figure 14B, lanes 2 and 4, respectively) and the hexahistidine tagged GleIF5CTD, GleIF1, and GleIF4E2 recombinant proteins (Figure 14B, lanes 3, 5, and 6, respectively) were also expressed and purified from *E. coli.*

Figure 13

Schematic Diagram of the Conserved Interactions between eIFβ and its Binding Partners

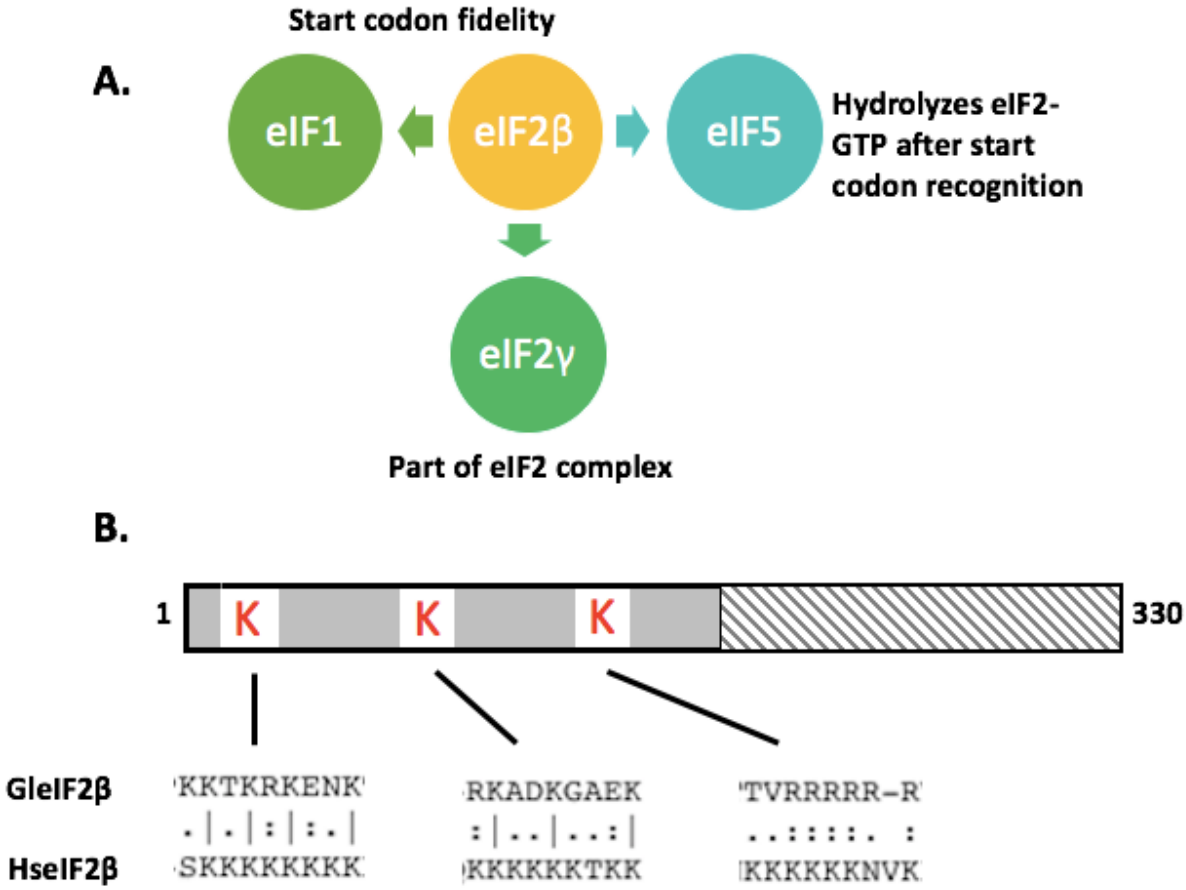

Note. Schematic representation showing conserved interactions of eukaryotic initiation factor 2β with eIF1, eIF5, and eIF2γ (A). The conservation of lysine-rich or K boxes (shown in red) between Giardia and human sequences of eIF2β is indicated (B). The eIF2β unstructured region is displayed in gray, and the structured region is characterized by the cross-hashed bar (B).

Figure 14

Coomassie Blue Stained Gel Electrophoresis of Purified Recombinant Proteins

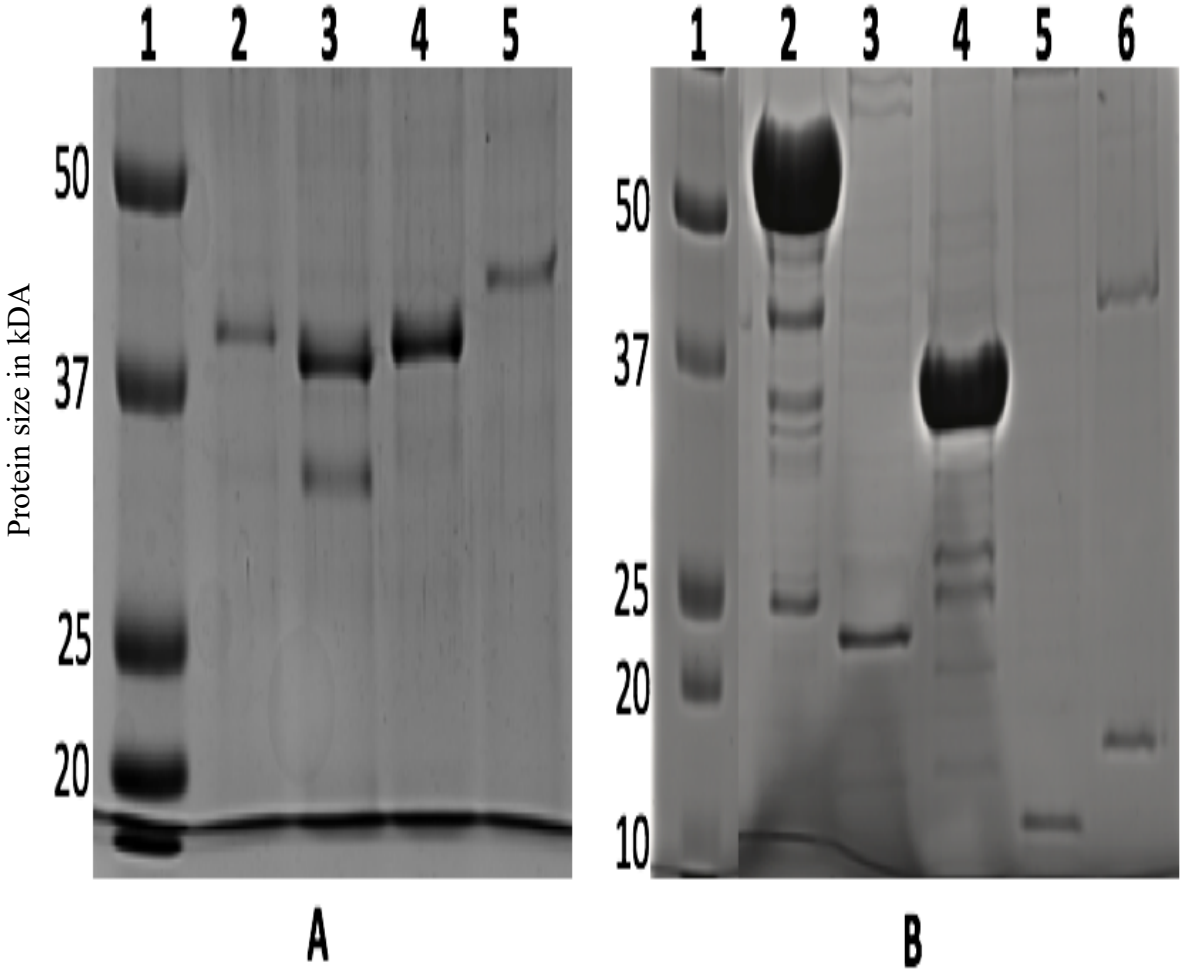

Note. Panel A shows a Coomassie-stained acrylamide gel of purified recombinant proteins of GleIF2β wildtype (lane 2), GleIF2β KR1 mutant (lane 3), GleIF2β KR2 mutant (lane 4), and GleIF2β KR3 mutant (lane 5). Coomassie-stained acrylamide gel (panel B) showing purified recombinant proteins of GST-GleIF5 (lane 2), GleIF5CTD-6his (lane 3), GST-GleIF1 (lane 4), GleIF1 -6his (lane 5), and GleIF4E2 (lane 6). In Figures A and B, individual protein lanes are numbered from one to five and from one to six, respectively.

The wildtype GleIF2β-6his displayed strong binding to GST-GleIF4E2 (Figure 7A, lane 2), GST-GleIF1 (Figure 15A, lane 3), and GST-GleIF5 (Figure 15A, lane 4). These results confirm the PPIs of GleIF2β with GleIF1, GleIF5, and GleIF4E2 as observed in yeast two-hybrid assays (Adedoja et al., 2020). Interestingly, GleIF2β KR1 mutant showed significantly decreased binding to both GST-GleIF4E2 (Figure 15B, lane 2) and GST-GleIF1 (Figure 15B, lane 3) but not to GST-GleIF5 (Figure 15B, lane 4) as compared to the wildtype controls (Figure 15A). The GleIF2β KR2 mutant did not bind at all to GST-GleIF4E2 (Figure 15C, lane 2), showed weak binding to GST-GleIF1 (Figure 15C, lane 3), but retained its strong binding affinity to GST-GleIF5 (Figure 15C, lane 4). However, the GleIF2β KR3 mutant did not bind to GST-GleIF4E2 (Figure 15D, lane 2) but displayed very weak binding to GST-GleIF1 (Figure 7D, lane 3) and GST-GleIF5 (Figure 15D, lane 4). As anticipated, the GST negative control did not bind to the wild type (Figure 15A, lane 1) and all the KR mutants (Figure 15B-D, lane 1).

These results show that the poorly conserved lysine and arginine patches in all three K boxes of the unstructured N terminal domain of the GleIF2β are important for PPIs with GleIF1 and GleIF4E2, while only the K3 box is important for binding to GleIF5. However, it is unclear if the residues in each box are directly involved in PPIs with these three proteins or are playing a role in maintaining unstructured protein conformation as lysine and arginine amino acids are negatively charged and thus tend to prevent local secondary structures. These results suggest that GleIF4E2, GleIF1, and GleIF5 bind to the N terminal domain of GleIF2β and hence may share a common binding site.

Figure 15

Binary Ppi between GleIF4E2, GleIF1, GleIF5 and GleIF2β-6his-WT and Mutants

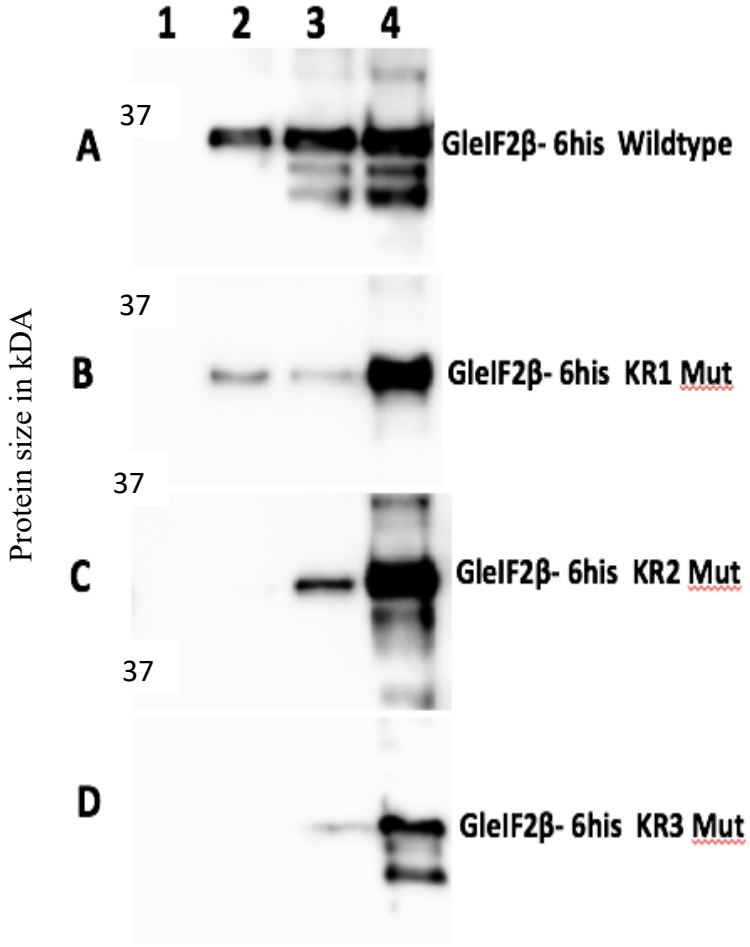

Note. Western blot analysis of binary protein-protein interaction between GST-GleIF4E2 (lane 2), GST-GleIF1 (lane 3), and GST-GleIF5 (lane 4) with GleIF2β -6His wildtype (panel A), KR1 (panel B), KR2 (panel C), and KR3 (panel D) mutants. GST alone (lane 1 in all panels) was tested against GleIF2β -6His wildtype and all KR mutants and served as a negative control. The 37 kDa size of the standard protein marker is indicated on the left. Individual protein lanes are numbered from one to four

Interaction between GleIF42 and GleIF2β is Competitively Favored over GleIF1-GleIF2β Interaction:

Having discovered that GleIF1 and GleIF4E2 bind to a common interface on GleIF2ß, we attempted to identify if a complex multifactor association could occur between GleIF1, GleIF4E2, and GleIF2β. A complex GST pull-down assay was performed using GST-GleIF1 as a bait protein and GleIF2β-6his and GleIF4E2-6his as prey proteins. As expected and consistent with previous observations and yeast-two hybrid assays, when GleIF2β-6his and GleIF4E2-6his proteins were incubated with GST-GleIF1 protein individually, only GleIF2β-6his showed binding to GST-GleIF1 (Figure 16, lane 4) but not GleIF4E2-6his (Figure 16, lane 3). Neither of these proteins showed nonspecific binding to GST alone (Figure 16, lanes 1 and 2). However, when both proteins GleIF2β-6his and GleIF4E2 were incubated simultaneously with GST-GleIF1, only GleIF2β-6his was able to bind GST-GleIF1 (Figure 16, lane 5), but the binding was moderate compared to the binding observed when GleIF2β-6his was added alone (Figure 16, lane 4). Interestingly, when GleIF2β-6his was initially incubated with GST-GleIF1 prior to adding GleIF4E2-6his to the mixture, the binding of GleIF2β-6his to GST-GleIF1 was significantly decreased (Figure 16, lane 6). These results suggest that GleIF4E2-6his competes with GleIF1 for binding to GleIF2β-6his, perhaps due to the difference in binding affinities of GleIF4E2 and GleIF1, GleIF4E2 can pull out bound GleIF2β-6his from GST-GleIF1. As GleIF4E2-6his was not detected in any of the binary complexes formed in this assay, it is reasonable to assume that a ternary complex association does not exist between GST-GleIF1, GleIF4E2-6his, and GleIF2β -6his.

Figure 16

Competitive Ppi between GST- GleIF1,GleIF4E2-his and GleIF2β-6his

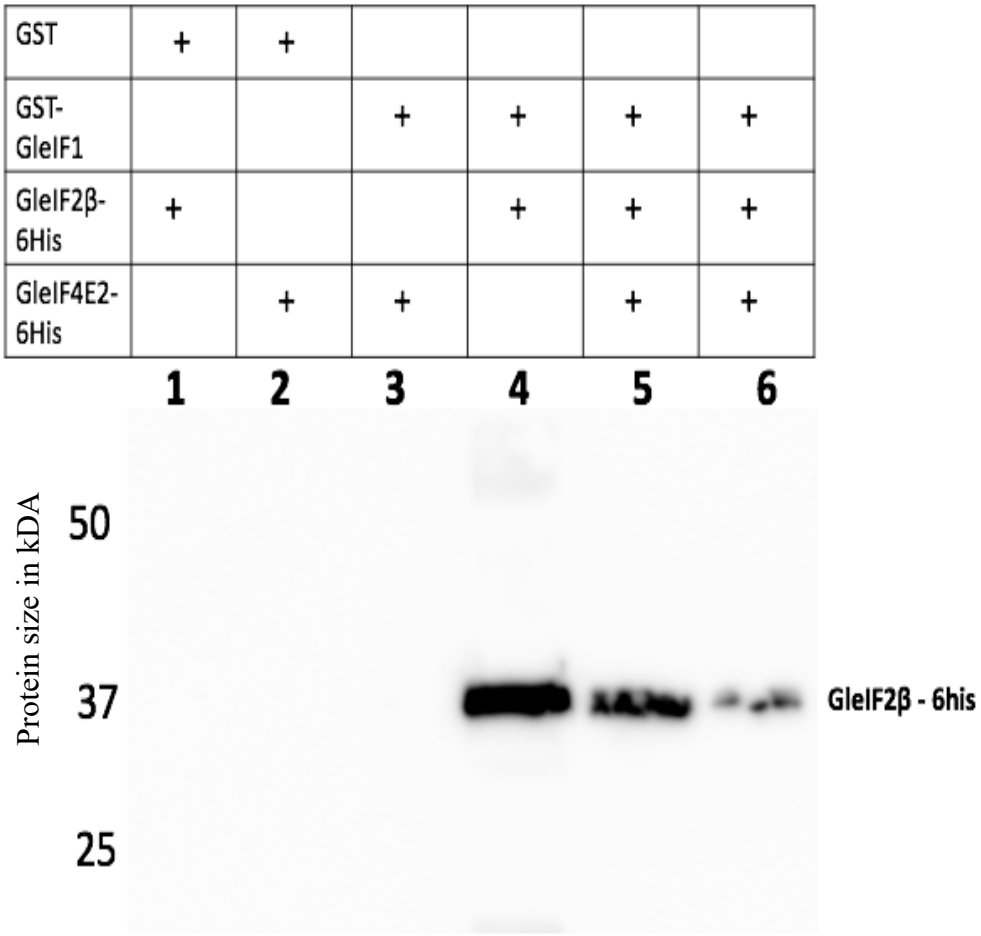

Note. GST-pull down assay to detect competitive or cooperative interaction between GST-GleIF1, GleIF2β-6his, and GleIF4E2-6his recombinant proteins. Anti-His antibody was used to detect the binding of his tagged proteins GleIF2β and GleIF4E2 to GST alone or to GST-GleIF1. GleIF2β-6his was incubated with GST alone (lane 1) or with GST-GleIF1 (lane 4), whereas GleIF4E2-6his was incubated with GST alone (lane 2) or with GST-GleIF1 (lane 3). To detect competitive or cooperative binding, GleIF2β-6his and GleIF4E2-6his were incubated simultaneously with GST-GleIF1 (lane 5) or incubated sequentially with initial incubation of GleIF2β-6his followed by incubation with GleIF4E2-6his (lane 6).

GleIF1 does not Compete out GleIF2β from GleIF4E2:

To further confirm that GleIF4E2 has a greater affinity than GleIF1 for binding to GleIF2β, competition assays were performed using GST-GleIF4E2 as a bait protein while GleIF1-6his and GleIF2β-6his were used as prey proteins. In this assay, as expected, GleIF2β-6his bound to GST-GleIF4E2, while GleIF1-6his did not (Figure 17, lanes 2 and 3, respectively) when added individually. Neither proteins showed nonspecific binding to the GST negative control (Figure 17, lanes 1 and 2). Slightly decreased binding of GleIF2β-6his to GST-GleIF4E2 was observed when added simultaneously with GleIF1-6his (Figure 17, lane 5). However, the binding of GleIF2β-6his to GST-GleF4E2 was unaffected when it was initially incubated with GST-GleIF4E2 prior to adding GleIF1-6his to the mixture (Figure 17, lane 6). These results suggest that GleIF1-6his cannot pull out bound GleIF2β-6his from GST-GleIF4E2, perhaps due to the weaker affinity of GleIF1-6his for bound GleIF2β-his.

Figure 17

Competitive Ppi between GST- GleIF4E2,GleIF1-his and GleIF2β-6his

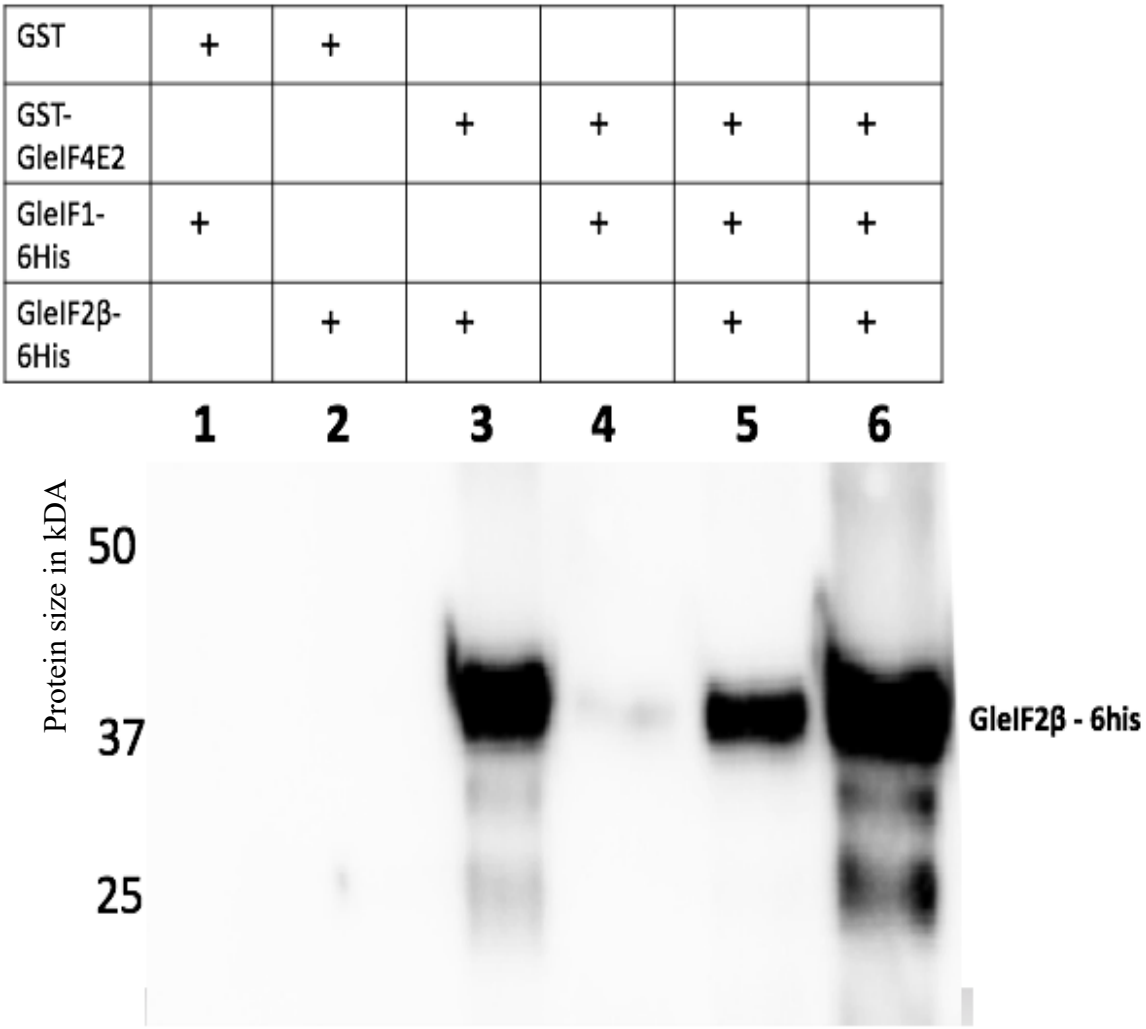

Note. GST-pull down assay to detect competitive or cooperative interaction between GST-GleIF4E2, GleIF2β-6his, and GleIF1-6his recombinant proteins. Anti-His antibody was used to detect the binding of his tagged proteins GleIF2β and GleIF1 to GST alone or to GST-GleIF1. GleIF1 was incubated with GST alone (lane 1) or with GST-GleIF4E2 (lane 4), whereas GleIF2β-6his was incubated with GST alone (lane 2) or with GST-GleIF4E2 (lane 3). To detect competitive or cooperative binding, GleIF2β-6his and GleIF1-6his were incubated simultaneously with GST-GleIF4E2 (lane 5) or incubated sequentially with initial incubation of GleIF2β-6his followed by incubation with GleIF1-6his (lane 6).

GleIF5 does not form a Complex with GleIF4E2 and GleIF2β:

Based on the results from mutagenesis of K boxes of GleIF2β (Figure 15), it is conceivable that GleIF4E2 and GleIF5 may also share a common binding site on GleIF2β. To determine if the binding of GleIF4E2 and GleIF5 to GleIF2β is competitive or cooperative, GST-pull-down assays were performed. In this assay, GST-GleIF5 was used as a bait protein, and GleIF2β-6his and GleIF4E2-6his were used as prey proteins. Consistent with the previous observations, GleIF2β-6his displayed a strong binding to GST-GleIF5 (Figure 18, lane 4), whereas GleIF4E2-6his failed to bind GST-GleIF5 (Figure 18, lane 3). A faint band corresponding to a 37kDa protein observed in lane 3 is due to a possible overflow of GleIF2β-6his from lane 4. It does not represent the binding of GleIF4E2-6his, which has a molecular weight of approximately 19 kDa (Figure 14B, lane 6). GleIF2β-6his and GleIF4E2-6his did not bind nonspecifically to GST negative control (Figure 18, lanes 1 and 2, respectively). When GleIF2β-6his and GleIF4E2 were added simultaneously to GST-GleIF5, only GleIF2β-6his was detected, but GleIF42-6his was not detected (Figure 18, lane 5), suggesting that GleIF4E2-6his does not form a ternary complex with GleIF2β and GleIF5. Interestingly, when GleIF2β-6his was incubated with GST-GleIF5 prior to adding GleIF4E2-6his to the mixtures, only GleIF2β-6his bound to GST-GleIF5 (Figure 18, lane 6), these results suggest that GleIF5 has a stronger affinity than GleIF4E2 for binding to GleIF2β, and once bound GleIF2β-6his cannot be dissociated from GST-GleIF5 by GleIF4E2-6his.

Figure 18

Competitive Ppi between GST- GleIF5,GleIF4E2-his and GleIF2β-6his

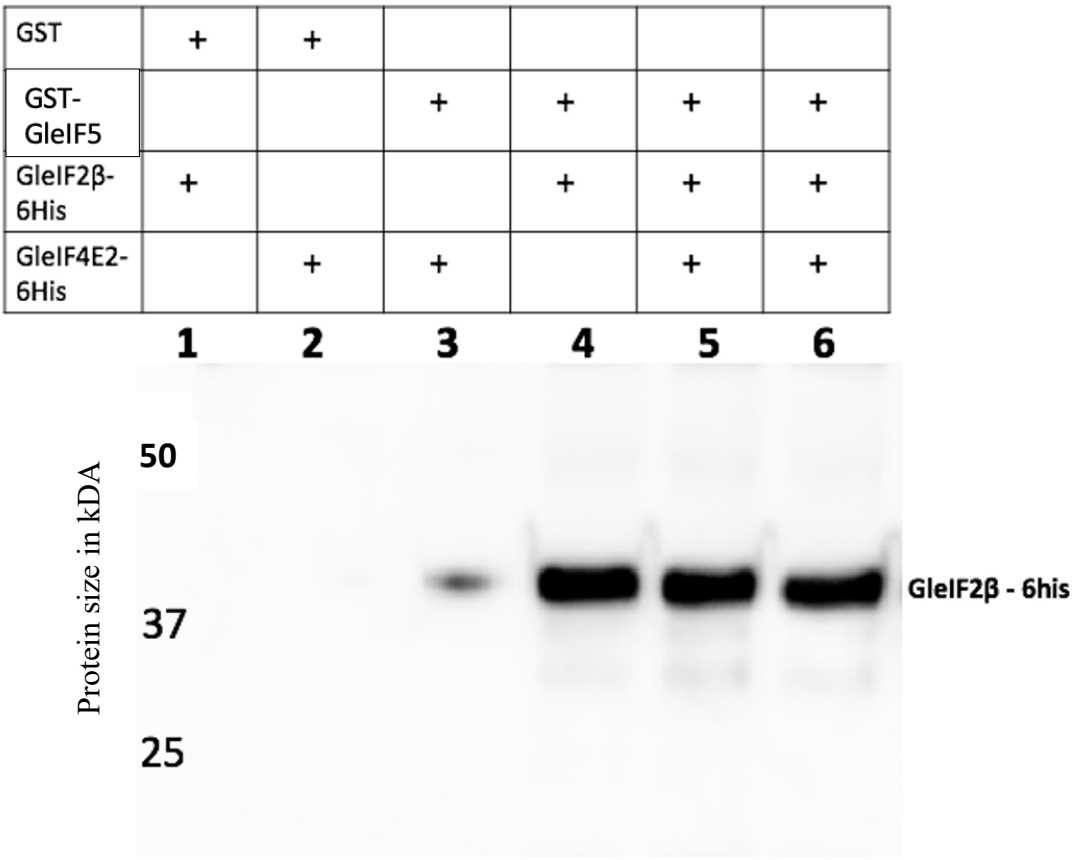

Note. GST-pull down assay to detect competitive or cooperative interaction between GST-GleIF5, GleIF2β-6his, and GleIF4E2-6his recombinant proteins. Anti-His antibody was used to detect the binding of his-tagged proteins GleIF2β and GleIF4E2 to GST alone or to GST-GleIF5. GleIF2β-6his was incubated with GST alone (lane 1) or with GST-GleIF5 (lane 4), whereas GleIF4E2-6his was incubated with GST alone (lane 2) or with GST-GleIF5 (lane 3). To detect competitive or cooperative binding, GleIF2β-6his and GleIF4E2-6his were incubated simultaneously with GST-GleIF5 (lane 5) or incubated sequentially with initial incubation of GleIF2β-6his followed by incubation with GleIF4E2-6his (lane 6).

GleIF1, GleIF2β and GleIF5 forms a Ternary Complex

The results summarized in Figure 15 suggest that GleIF1 and GleIF5 share a common binding interface in GleIF2β. GST-pull-down assays were performed to determine if GleIF1, GleIF2β , and GleIF5 form a ternary complex. In this assay, GST-GleIF1 was used as a bait protein, while GleIF2β-6his and GleIF5 CTD-6his were used as prey proteins. In previous experiments, GleIF2β-6his was bound to GST-GleIF1 (Figure 19, lane 3) but not to GST alone (Figure 19, lane 1). Similarly, GleIF5 CTD-6his was attached to GST-GleIF1 (Figure 11, lane 4) but not GST alone (Figure 19, lane 2). However, when both GleIF2β-6his and GleIF5CTD were incubated simultaneously, they both bound and formed a ternary complex with GST-GleIF1. These results indicate that GleIF1 and GleIF5 can cooperatively bind to GleIF2β to form a multi-factor complex, as observed in higher-order eukaryotes.

Figure 19

Cooperative Ppi between GST-GleIF1, GleIF5C-6his, and GleIF2β-6his

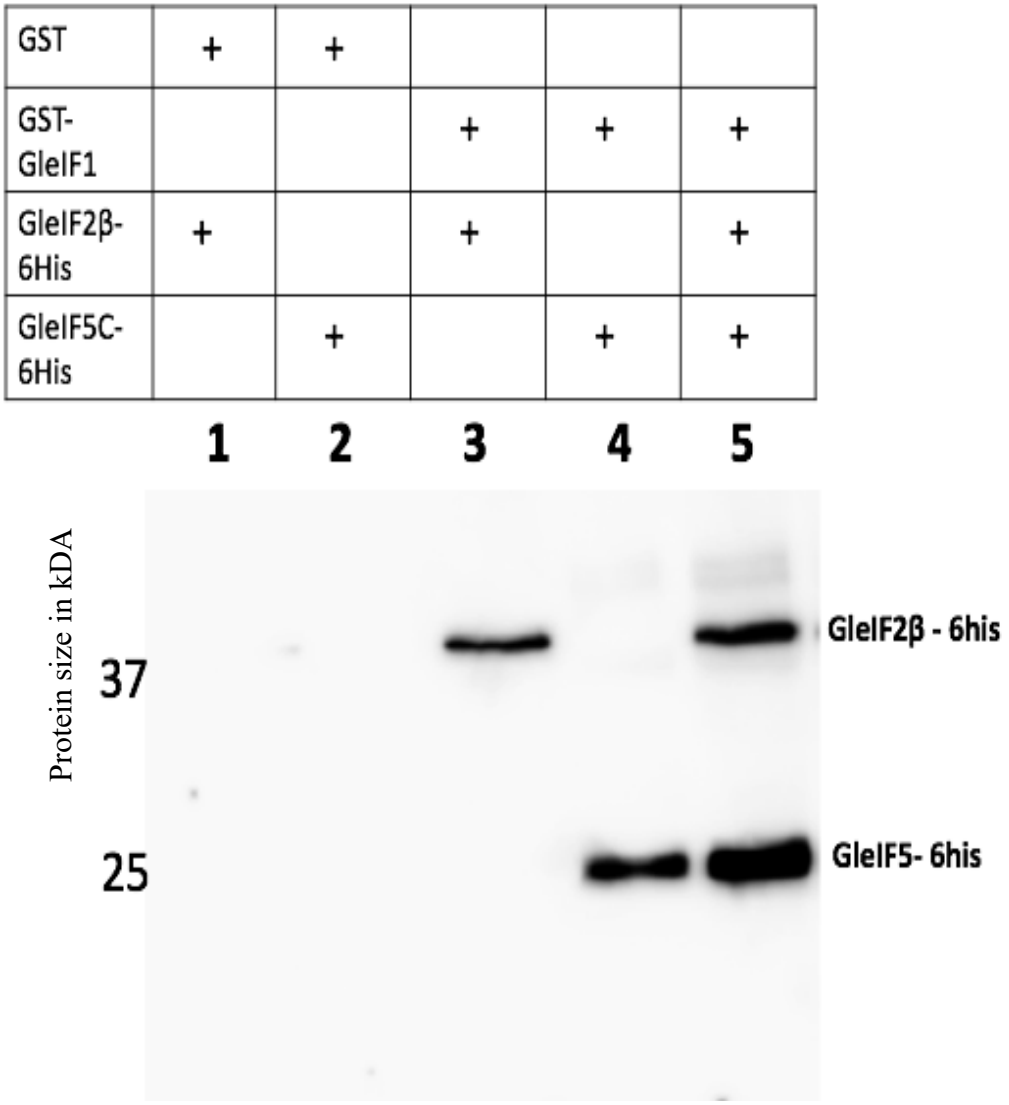

Note. GST-pull down assay to detect competitive or cooperative interaction between GST-GleIF1, GleIF2β-6his, and GleIF5CTD-6his recombinant proteins. Anti-His antibody was used to detect the binding of his tagged proteins GleIF2β and GleIF5CTD to GST alone or to GST-GleIF1. GleIF2β-6his was incubated with GST alone (lane 1) or with GST-GleIF1 (lane 3), whereas GleIF5CTD-6his was incubated with GST alone (lane 2) or with GST-GleIF1 (lane 4). To detect competitive or cooperative binding, GleIF2β-6his and GleIF5CTD-6his were incubated simultaneously with GST-GleIF1 (lane 5).

CHAPTER IV

Discussion and Conclusion

The recruitment of the ribosome to the 5'end of the mRNA is a critical aspect of the translation mechanism. eIF4G, a subunit of the eIF4F complex, stimulates this process through interaction with eIF4A, which unwinds the secondary structures on the mRNA and produces a smooth single-stranded landing path for the ribosome (Figure 20). Direct physical interactions between eIF4G with eIF3 or eIF5 of the preinitiation complex facilitate PIC recruitment. There is no identified eIF4G homolog in Giardia. The absence of an eIF4G homolog provided the foundational question in the studies performed by Adedoja et al. (2020) and the rationale for their yeast two-hybrid experiments. Their study reported a novel protein-protein interaction between GleIF4E2 and GleIF2β. This unprecedented interaction may be sufficient in recruiting the PIC to the 5'end of the mRNA. This study extensively analyzed purified recombinant Giardia initiation factors using GST affinity chromatography pull-down assay to elucidate the molecular mechanism of ribosome recruitment in Giardia. The results generated from the pull-down assays validate the observed protein-protein interaction between GleIF4E2 with GleIF2β in yeast two-hybrid systems(Adedoja et al., 2020). The interaction between GleIF4E2 and GleIF2β was further characterized to identify the amino-acid residues mediating the protein-protein interaction and the significance of the unstructured regions of GleIF2β.

Further evidence from the GST pull-down has been provided to support the proposed mechanistic overview of Giardia translation initiation (Figure 21).

The mechanistic overview of the Giardia translation initiation process remains unclear. It is believed that Giardia may employ a straightforward initiation process independent of scanning. The relatively short 5'UTR brings the start codon in proximity with capped mRNA. The short 5'UTR is unlikely to be sequestered in secondary structures that may impair PIC recruitment. Cryo-EM studies have provided insights into the structural organization of the translation initiation complex in yeast. eIF2β was found close to the mRNA entry channel of the ribosome, and its helix-turn-helix domain (HTH) forms contacts with eIF1 to maintain an open scanning competent conformation. Therefore, the observed interaction between GleIF4E2 with GleIF2β could be implicated in recruiting the mRNA to the entry channel of the ribosome.

eIF4E is structurally and functionally conserved throughout evolution. Human and Giardia homologs have a 28.8% sequence similarity. In comparison, human and yeast homologs have 36.6% sequence similarity. The Giardia eIF4E2 encodes 168 amino acids. Mutating residues L12, F45, and F46 into alanines were found to disrupt the observed protein-protein interaction between GleIF4E2 with GeIF2β completely. In higher eukaryotes, the dorsal surface of eIF4E mediates eIF4G binding, while the lateral surface mediates 4E-binding proteins (Igreja et al., 2014). Interestingly, the mutated residues on the dorsal surface of GleIF4E2 are similar to the hydrophobic residues on the dorsal side of eIF4E that mediate the binding of eIF4G. Hence, GeIF2β binding to GleIF4E2 may provide a function identical to eIF4G. The observed disruption of protein-protein is congruent with previous data from yeast two-hybrid studies(Adedoja et al., 2020).

Having determined the amino acid residues on the dorsal surface of GleIF4E2 that mediate binding with GeIF2β, we determined the functional role of GleIF4E2 and the effects of mutations on the protein structure. Studies by Li & Wang (2005) determined the functional role of GleIF4E2 as a cap-binding protein. Using *in vitro* and *in vivo* assays, they demonstrated that the m^7GpppN-cap is the cap of Giardia mRNA, and GleIF4E2 is the functional cap-binding protein involved in translation initiation. Similarly, m^7GTP sepharose pull-down was performed to verify the functional role of both GleIF4E2 wildtype and mutant proteins. It was observed that both wildtype and mutant proteins maintained their ability to bind to the m^7GTP cap analog. The Swiss Model was used to generate the three-dimensional structure of the proteins using their respective wildtype and mutated amino acid sequences. No changes were observed in the protein structures. This observation implies that mutations in the dorsal surface of GleIF4E2 did not induce a change in protein structure, and the ZDOCK predicted residues L12, F45, and F46 are crucial for the interaction of GleIF4E2 with GeIF2β.

The beta subunit of eIF2 mediates interactions with several components of the preinitiation complex through its unstructured polylysine stretches. Data reported by Laurino et al. (1999) provided evidence for the mRNA binding activity of eIF2β. They reported that removing the conserved lysine residues conferred a suppression of the initiation phenotype, which indicates that the lysine residues are required *in vivo*. Consistent with their results, mutating the conserved stretches of lysine and arginine patches in GleIF2β into alanines did not replicate the wild-type function of GleIF2β in binding with GleIF4E2. The finding that all GleIF2β KR mutants associate with GleIF5 and KR1 and KR2 mutants associate with GleIF1 may suggest that the GeIF2β may play a

dual role in interacting with GleIF4E2 and other components of the preinitiation complex to recruit the ribosome to the 5'end of the mRNA. Thus, the lysine/arginine patches may function as a facilitator in GleIF4E2 binding and aid in the secondary binding to GleIF5 and GleIF1.

The above data confirm and validate the protein-protein interaction between GleIF4E2 and GeIF2β. The proposed consequence of this interaction is the recruitment of the ribosome onto the 5'end of the mRNA. Ribosomal recruitment is a multifactor process that requires an interplay between several host initiation factors that toggles the PIC between opened and closed conformations. Cryo-EM studies of yeast reconstituted 48S PICS presented by Llácer et al. (2015) observed contacts between eIF2β with eIF1 and eIF1A on the body with $tRNA_i$ on the 40S head. These contacts stabilize eIF1 and the ternary complex between eIF2-GTP and Met-$tRNA_i$ before AUG: anticodon recognition in the P site. Thus, eIF2β contacts with eIF1 and $tRNA_i$ are a bridging interaction stabilizing the open conformation and aiding PIC recruitment. Consistent with this observation, GeIF2β was found to form contacts with GleIF1 which presumably stabilizes the PIC in an open conformation to enable accurate start codon recognition. Substitutions at both interfaces destabilizing eIF2β/eIF1 contacts were found to promote inaccurate start codon selection in yeast cells. This further reestablishes that eIF2β/eIF1 contacts denote an open conformation of the 48S PIC, and destabilization of these contacts induces rearrangement into a closed complex without a perfect start codon.

Interestingly, GleIF4E2 was found to destabilize GeIF2β from GleIF1 competitively. Since the network of eIF2β interaction with eIF1, eIF1A, and $tRNA_i$ impede mRNA insertion into the mRNA channel at the P site, eIF2β is likely repositioned to allow

mRNA recruitment(Llácer et al., 2015). This supports our hypothesis that the observed destabilization of GeIF2β/GleIF1 contacts caused by GleIF4E2 may promote transient repositioning of GeIF2β, allowing mRNA recruitment and that GeIF2β serves as a barrier to mRNA recruitment and release. This function is unique to GeIF2β since a similar observation was not seen when GeIF2β was replaced with GleIF5.

eIF2β interacts with eIF5 via the CTD of eIF5. eIF5 is a GTPase activating protein that promotes the hydrolysis of eIF2-GTP after AUG-codon recognition. This triggers the dissociation of the eIF5/eIF2•GDP complex from the PIC prior to 60S joining. eIF5 performs a secondary inhibitory function termed GDP dissociation inhibitor activity (GDI) which prevents the spontaneous release of GDP from eIF2. GDI activity requires the physical protein-protein interaction between eIF5-CTD with eIF2β. Mutations within eIF5-CTD that weaken eIF5 binding to eIF2 were found to eliminate GDI (Jennings et al., 2016). These data suggest that eIF2β performs a critical role in maintaining eIF5 GDI. This may explain the strong binding interaction observed between GleIF2β with GleIF5. GleIF2β may play a mechanistic role in PIC recruitment and GDP dissociation. Thus, the observed interaction between GleIF2β and GleIF5 may act as a molecular clamp that inhibits GDP release. Following PIC recruitment by GleIF4E2, GleIF2β is destabilized from GleIF1, causing rearrangement into a closed PIC and the coupled release of inorganic phosphate and GDP.

The formation of a stable ternary complex between GleIF1, GeIF2β, and GleIF5 further supports this proposed mechanism of *Giardia* translation (Figure 21). In higher eukaryotes, the interaction between eIF1 and eIF5 manipulates the closed and open states of the AUG or UUG-bound PIC. In yeast, accurate start recognition is mediated by a similar

interplay between eIF5, eIF1, and all three subunits of eIF2(Asano et al., 2000). Since Giardia may utilize a straightforward initiation mechanism that does not rely on scanning, it is possible that a pre-formed complex of GleIF1, GleIF2β, and GleIF5 may independently associate with the 40S ribosome and facilitate a rapid assemble of the preinitiation complex. This fits perfectly into the proposed mechanistic picture of Giardia initiation, where after the rapid formation of the PIC, GleIF4E2 binds to GleIF2β in the PIC to facilitate the recruitment of the ribosome. Once bound near the cap, the initiator tRNA is paired with the AUG anticodon, positioned near the capped mRNA. The interaction between GleIF4E2 with GeIF2β, however, destabilizes the GleIF1/GleIF2β complex, disrupting the proposed molecular clamp and allowing GleIF5 to induce GDP conversion via gated phosphate release. GleIF2-GDP and GelF1 are dissociated from the complex to enable the joining of the large 60S subunit catalyzed by GleIF5B. This forms an elongation-competent 80S complex with the initiator tRNA (Met-tRNA$_i$) position in the P site and is ready to commence the next step of protein synthesis.

Areas of further research may involve cryo-EM to validate this proposed hypothesis. GleIF4E2 mutants can be investigated to assess the effect of these mutations *in vivo*. These answers may provide valuable insight into the mechanistic overview of Giardia translation initiation and potential ligand site for pharmacotherapy.

Figure 20

Schematic Cartoon of Canonical Translation Initiation in Eukaryotes

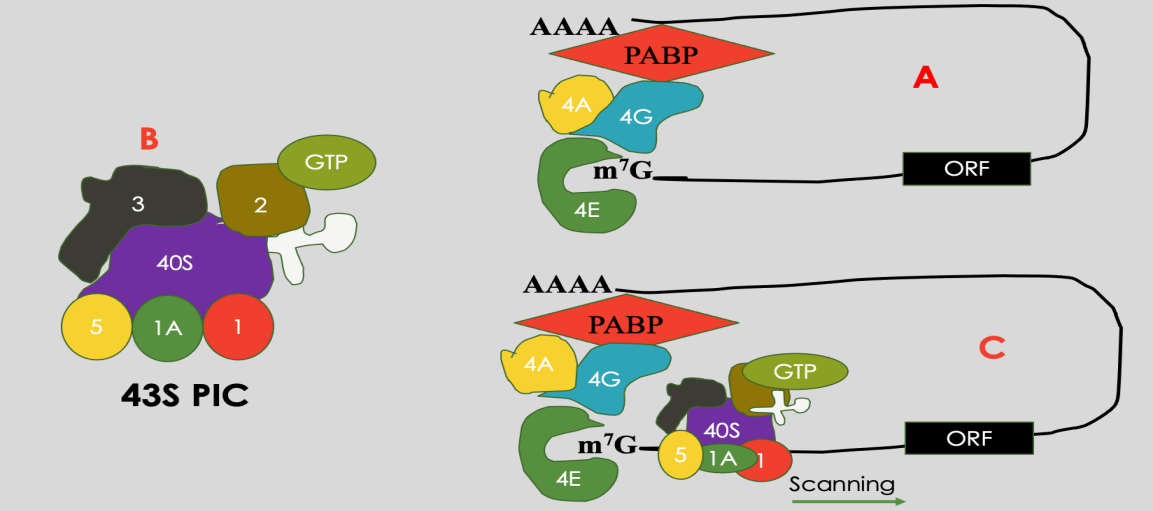

Note. In diagram A, the mRNA is circularized by its interaction with the translation initiation factors. The eIF4F complex binds to the (m^7G) at the 5' end of the mRNA. In diagram B, the 43S pre-initiation complex is assembled. This comprises the 40S ribosomal subunit, eIF3, eIF1, eIF1A, eIF5, and the ternary complex consisting of eIF2-GTP-Met-tRNAi. In diagram C, the PIC is recruited to the 5'end of the mRNA through interaction between the eIF4F complex and eIF3. The PIC scans the mRNA for the AUG start codon.

Figure 21

Schematic Cartoon of the Proposed Translation Initiation Mechanism in Giardia

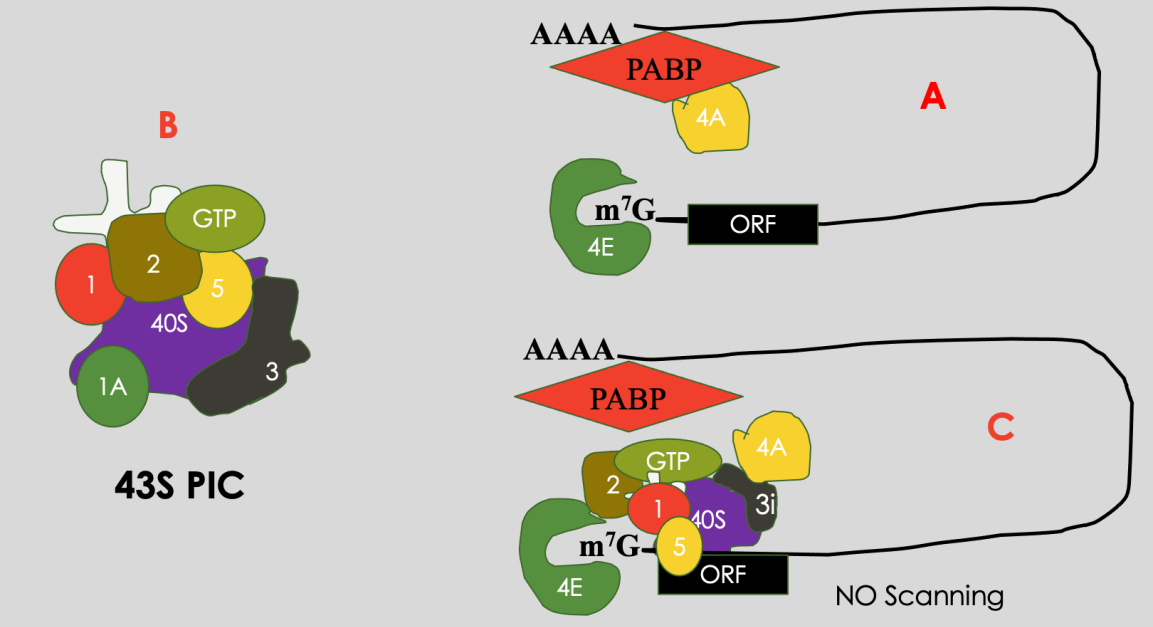

Note. In diagram A, the GleIF4E2 binds to the 5'end of the mRNA. In diagram B, a preformed complex consisting of GleIF1, GleIF5, and GleIF2 associates with the 40S subunit to form the 43S PIC. In diagram C, the PIC is recruited to the AUG-start codon through interactions between GleIF4E2 and GleIF2β. There is no scanning since the AUG codon is near the 5'UTR.

REFERENCES

Adam, E. A., Yoder, J. S., Gould, L. H., Hlavsa, M. C., & Gargano, J. W. (2016). Giardiasis outbreaks in the United States, 1971-2011. In *Epidemiology and Infection* (Vol. 144, Issue 13). https://doi.org/10.1017/S0950268815003040

Adam, R. D. (2021). Giardia duodenalis: Biology and Pathogenesis. In *Clinical Microbiology Reviews* (Vol. 34, Issue 4). https://doi.org/10.1128/CMR.00024-19

Adam, R. D., Dahlstrom, E. W., Martens, C. A., Bruno, D. P., Barbian, K. D., Ricklefs, S. M., Hernandez, M. M., Narla, N. P., Patel, R. B., Porcella, S. F., & Nash, T. E. (2013). Genome sequencing of Giardia lamblia genotypes A2 and B isolates (DH and GS) and comparative analysis with the genomes of Genotypes A1 and E (WB and pig). *Genome Biology and Evolution*, *5*(12). https://doi.org/10.1093/gbe/evt197

Adedoja, A. N., McMahan, T., Neal, J. P., Hamal Dhakal, S., Jois, S., Romo, D., Hull, K., & Garlapati, S. (2020a). Translation initiation factors GleIF4E2 and GleIF4A can interact directly with the components of the pre-initiation complex to facilitate translation initiation in Giardia lamblia. *Molecular and Biochemical Parasitology*, *236*. https://doi.org/10.1016/j.molbiopara.2020.111258

Aitken, C. E., & Lorsch, J. R. (2012). A mechanistic overview of translation initiation in eukaryotes. In *Nature Structural and Molecular Biology* (Vol. 19, Issue 6). https://doi.org/10.1038/nsmb.2303

Amahmid, O., Asmama, S., & Bouhoum, K. (1999). The effect of wastewater reuse in irrigation on the contamination level of food crops by Giardia cysts and Ascaris eggs. *International Journal of Food Microbiology*, *49*(1–2). https://doi.org/10.1016/S0168-1605(99)00058-6

Anil Thakur, Laura Marler, & Alan G Hinnebusch. (2019). A network of eIF2β interactions with eIF1 and Met-tRNAi promotes accurate start codon selection by the translation preinitiation complex. *National Library of Medicine National Center for Biotechnology Information*. https://pubmed.ncbi.nlm.nih.gov/30576497/

Asano, K., Clayton, J., Shalev, A., & Hinnebusch, A. G. (2000). A multifactor complex of eukaryotic initiation factors, eIF1, eIF2, eIF3, eIF5, and initiator tRNA(Met) is an important translation initiation intermediate in vivo. *Genes and Development*, *14*(19). https://doi.org/10.1101/gad.831800

Awasthi, S., & Pande, V. K. (1997). Prevalence of malnutrition and intestinal parasites in preschool slum children in Lucknow. *Indian Pediatrics*, *34*(7).

Beer, K. D., Collier, S. A., Du, F., & Gargano, J. W. (2017). Giardiasis diagnosis and treatment practices among commercially insured persons in the United States. *Clinical Infectious Diseases*, *64*(9). https://doi.org/10.1093/cid/cix138

Benedict, K. M., Reses, H., Vigar, M., Roth, D. M., Roberts, V. A., Mattioli, M., Cooley, L. A., Hilborn, E. D., Wade, T. J., Fullerton, K. E., Yoder, J. S., & Hill, V. R. (2017). Surveillance for Waterborne Disease Outbreaks Associated with Drinking Water — United States, 2013–2014. *MMWR. Morbidity and Mortality Weekly Report*, *66*(44). https://doi.org/10.15585/mmwr.mm6644a3

Benelli, D., & Londei, P. (2011). Translation initiation in Archaea: Conserved and domain-specific features. *Biochemical Society Transactions*, *39*(1). https://doi.org/10.1042/BST0390089

Bruce W. Furness, M. D., Michael J. Beach, Ph. D., & Jacquelin M. Roberts. (2000). Giardiasis Surveillance --- United States, 1992--1997. *National Library of Medicine*. https://pubmed.ncbi.nlm.nih.gov/10955980/

Budu-Amoako, E., Greenwood, S. J., Dixon, B. R., Barkema, H. W., & McClure, J. T. (2011). Foodborne illness associated with Cryptosporidium and Giardia from livestock. In *Journal of Food Protection* (Vol. 74, Issue 11). https://doi.org/10.4315/0362-028X.JFP-11-107

CDC. (2013). *CDC - Giardia*. CDC.

Coffey, C. M., Collier, S. A., Gleason, M. E., Yoder, J. S., Kirk, M. D., Richardson, A. M., Fullerton, K. E., & Benedict, K. M. (2021). Evolving Epidemiology of Reported Giardiasis Cases in the United States, 1995-2016. *Clinical Infectious Diseases*, *72*(5). https://doi.org/10.1093/cid/ciaa128

de Smit, M. H., & van Duin, J. (1990). Secondary structure of the ribosome binding site determines translational efficiency: A quantitative analysis. *Proceedings of the National Academy of Sciences of the United States of America*, *87*(19). https://doi.org/10.1073/pnas.87.19.7668

De-Chao, Y., Wang, A. L., Botka, C. W., & Wang, C. C. (1998). Protein synthesis in Giardia lamblia may involve interaction between a downstream box (DB) in mRNA and an anti-DB in the 16S-like ribosomal RNA. *Molecular and Biochemical Parasitology*, *96*(1–2). https://doi.org/10.1016/S0166-6851(98)00126-1

Delahunty, C. M., & Yates, J. R. (2019). Protein-protein interactions. In *Proteomics for Biological Discovery*. https://doi.org/10.1002/9781119081661.ch5

Dingsdag, S. A., & Hunter, N. (2018). Metronidazole: An update on metabolism, structure-cytotoxicity and resistance mechanisms. *Journal of Antimicrobial Chemotherapy*, *73*(2). https://doi.org/10.1093/jac/dkx351

Dobell, C. (1920). The Discovery of the Intestinal Protozoa of Man. *Proceedings of the Royal Society of Medicine*, *13*(sect_hist_med). https://doi.org/10.1177/003591572001301601

Escobedo, A. A., Almirall, P., Alfonso, M., Cimerman, S., & Chacín-Bonilla, L. (2014). Sexual transmission of giardiasis: A neglected route of spread? In *Acta Tropica* (Vol. 132, Issue 1). https://doi.org/10.1016/j.actatropica.2013.12.025

Fields, S., & Song, O. K. (1989). A novel genetic system to detect protein-protein interactions. *Nature*, *340*(6230). https://doi.org/10.1038/340245a0

Fraser, D., Bilenko, N., Deckelbaum, R. J., Dagan, R., El-On, J., & Naggan, L. (2000). Giardia lamblia carriage in Israeli bedouin infants: Risk factors and consequences. *Clinical Infectious Diseases*, *30*(3). https://doi.org/10.1086/313722

French, S. L., Santangelo, T. J., Beyer, A. L., & Reeve, J. N. (2007). Transcription and translation are coupled in Archaea. *Molecular Biology and Evolution*, *24*(4). https://doi.org/10.1093/molbev/msm007

Gardner, T. B., & Hill, D. R. (2001). Treatment of giardiasis. In *Clinical Microbiology Reviews* (Vol. 14, Issue 1). https://doi.org/10.1128/CMR.14.1.114-128.2001

Gualerzi, C. O., & Pon, C. L. (2015). Initiation of mRNA translation in bacteria: Structural and dynamic aspects. In *Cellular and Molecular Life Sciences* (Vol. 72, Issue 22). https://doi.org/10.1007/s00018-015-2010-3

Guimarães, S., & Sogayar, M. I. L. (2002). Detection of anti-Giardia lamblia serum antibody among children of day care centers. *Revista de Saude Publica*, *36*(1). https://doi.org/10.1590/S0034-89102002000100010

Halliez, M. C. M., & Buret, A. G. (2013). Extra-intestinal and long term consequences of Giardia duodenalis infections. In *World Journal of Gastroenterology* (Vol. 19, Issue 47). https://doi.org/10.3748/wjg.v19.i47.8974

Hashimoto, T., Sánchez, L. B., Shirakura, T., Müller, M., & Hasegawa, M. (1998). Secondary absence of mitochondria in Giardia lamblia and Trichomonas vaginalis revealed by valyl-tRNA synthetase phylogeny. *Proceedings of the*

National Academy of Sciences of the United States of America, *95*(12). https://doi.org/10.1073/pnas.95.12.6860

Hinnebusch, A. G., & Lorsch, J. R. (2012). The mechanism of eukaryotic translation initiation: New insights and challenges. *Cold Spring Harbor Perspectives in Biology*, *4*(10). https://doi.org/10.1101/cshperspect.a011544

Hlavsa, M. C., Aluko, S. K., Miller, A. D., Person, J., Gerdes, M. E., LeeMSPH, S., LacoMS, J. P., Hannapel, E. J., & Hill, V. R. (2021). Outbreaks Associated with Treated Recreational Water —United States, 2015–2019. *MMWR Recommendations and Reports*, *70*(20). https://doi.org/10.15585/mmwr.mm7020a1

Hopkins, R. S., & Juranek, D. D. (1991). Acute giardiasis: An improved clinical case definition for epidemiologic studies. *American Journal of Epidemiology*, *133*(4). https://doi.org/10.1093/oxfordjournals.aje.a115894

Igreja, C., Peter, D., Weiler, C., & Izaurralde, E. (2014). 4E-BPs require non-canonical 4E-binding motifs and a lateral surface of eIF4E to repress translation. *Nature Communications*, *5*. https://doi.org/10.1038/ncomms5790

Jackson, R. J., Hellen, C. U. T., & Pestova, T. v. (2010). The mechanism of eukaryotic translation initiation and principles of its regulation. In *Nature Reviews Molecular Cell Biology* (Vol. 11, Issue 2). https://doi.org/10.1038/nrm2838

Jangra, M., Dutta, U., Shah, J., Thapa, B. R., Nada, R., Gupta, N., Sehgal, R., Sharma, V., & Khurana, S. (2020). Role of Polymerase Chain Reaction in Stool and Duodenal Biopsy for Diagnosis of Giardiasis in Patients with Persistent/Chronic Diarrhea. *Digestive Diseases and Sciences*, *65*(8). https://doi.org/10.1007/s10620-019-06042-2

Jennings, M. D., Kershaw, C. J., White, C., Hoyle, D., Richardson, J. P., Costello, J. L., Donaldson, I. J., Zhou, Y., & Pavitt, G. D. (2016). eIF2β is critical for eIF5-mediated GDP-dissociation inhibitor activity and translational control. *Nucleic Acids Research*, *44*(20), 9698–9709. https://doi.org/10.1093/nar/gkw657

Johnson, A. G., Grosely, R., Petrov, A. N., & Puglisi, J. D. (2017). Dynamics of IRES-mediated translation. In *Philosophical Transactions of the Royal Society B: Biological Sciences* (Vol. 372, Issue 1716). https://doi.org/10.1098/rstb.2016.0177

Keegan, L., Gill, G., & Ptashne, M. (1986). Separation of DNA binding from the transcription-activating function of a eukaryotic regulatory protein. *Science*, *231*(4739). https://doi.org/10.1126/science.3080805

Keller, D. M., Zeng, S. X., & Lu, H. (2003). Interaction of p53 with cellular proteins. *Methods in Molecular Biology (Clifton, N.J.)*, *234*. https://doi.org/10.1385/1-59259-408-5:121

Kim, S. Y., & Hakoshima, T. (2019). GST Pull-Down Assay to Measure Complex Formations. In *Methods in Molecular Biology* (Vol. 1893). https://doi.org/10.1007/978-1-4939-8910-2_20

Knodler, L. A., Svärd, S. G., Silberman, J. D., Davids, B. J., & Gillin, F. D. (1999). Developmental gene regulation in Giardia lamblia: First evidence for an encystation-specific promoter and differential 5' mRNA processing. *Molecular Microbiology*, *34*(2). https://doi.org/10.1046/j.1365-2958.1999.01602.x

Kozak, M. (2005). Regulation of translation via mRNA structure in prokaryotes and eukaryotes. In *Gene* (Vol. 361, Issues 1–2). https://doi.org/10.1016/j.gene.2005.06.037

Lalle, M., & Hanevik, K. (2018). Treatment-refractory giardiasis: Challenges and solutions. In *Infection and Drug Resistance* (Vol. 11). https://doi.org/10.2147/IDR.S141468

Laurino, J. P., Thompson, G. M., Pacheco, E., & Castilho, B. A. (1999). The β Subunit of Eukaryotic Translation Initiation Factor 2 Binds mRNA through the Lysine Repeats and a Region Comprising the C 2 -C 2 Motif . *Molecular and Cellular Biology*, *19*(1). https://doi.org/10.1128/mcb.19.1.173

Lee, S. H., Levy, D. A., Craun, G. F., Beach, M. J., & Calderon, R. L. (2002). Surveillance for waterborne-disease outbreaks--United States, 1999-2000. *Morbidity and Mortality Weekly Report. Surveillance Summaries (Washington, D.C. : 2002)*, *51*(8).

Lengerich, E. J., Addiss, D. G., & Juranek, D. D. (1994). Severe giardiasis in the united states. *Clinical Infectious Diseases*, *18*(5). https://doi.org/10.1093/clinids/18.5.760

Li, L., & Wang, C. C. (2004). Capped mRNA with a Single Nucleotide Leader Is Optimally Translated in a Primitive Eukaryote, Giardia lamblia. *Journal of Biological Chemistry*, *279*(15). https://doi.org/10.1074/jbc.M309879200

Li, L., & Wang, C. C. (2005a). Identification in the ancient protist Giardia lamblia of two eukaryotic translation initiation factor 4E homologues with distinctive functions. *Eukaryotic Cell*, *4*(5). https://doi.org/10.1128/EC.4.5.948-959.2005

Llácer, J. L., Hussain, T., Marler, L., Aitken, C. E., Thakur, A., Lorsch, J. R., Hinnebusch, A. G., & Ramakrishnan, V. (2015). Conformational Differences between Open and Closed States of the Eukaryotic Translation Initiation Complex. *Molecular Cell*, *59*(3). https://doi.org/10.1016/j.molcel.2015.06.033

MAEDA, K., OSATO, T., & UMEZAWA, H. (1953). A new antibiotic, azomycin. *The Journal of Antibiotics*, *6*(4).

Milon, P., Konevega, A. L., Gualerzi, C. O., & Rodnina, M. v. (2008). Kinetic Checkpoint at a Late Step in Translation Initiation. *Molecular Cell*, *30*(6). https://doi.org/10.1016/j.molcel.2008.04.014

Milón, P., Maracci, C., Filonava, L., Gualerzi, C. O., & Rodnina, M. v. (2012). Real-time assembly landscape of bacterial 30S translation initiation complex. *Nature Structural and Molecular Biology*, *19*(6). https://doi.org/10.1038/nsmb.2285

Monis, P. T., Caccio, S. M., & Thompson, R. C. A. (2009). Variation in Giardia: towards a taxonomic revision of the genus. In *Trends in Parasitology* (Vol. 25, Issue 2). https://doi.org/10.1016/j.pt.2008.11.006

Nakagawa, S., Niimura, Y., Miura, K. I., & Gojobori, T. (2010). Dynamic evolution of translation initiation mechanisms in prokaryotes. *Proceedings of the National Academy of Sciences of the United States of America*, *107*(14), 6382–6387. https://doi.org/10.1073/pnas.1002036107

Noel Dunn, & Andrew L. Juergens. (2022). *Giardiasis*. https://www.ncbi.nlm.nih.gov/books/NBK513239/

Nooren, I. M. A., & Thornton, J. M. (2003). Diversity of protein-protein interactions. In *EMBO Journal* (Vol. 22, Issue 14). https://doi.org/10.1093/emboj/cdg359

Ortega, Y. R., & Adam, R. D. (1997). Giardia: overview and update. *Clinical Infectious Diseases*, *25*(3). https://doi.org/10.1086/513745

Painter, J. E., Collier, S. A., & Gargano, J. W. (2017). Association between Giardia and arthritis or joint pain in a large health insurance cohort: Could it be reactive arthritis? *Epidemiology and Infection*, *145*(3). https://doi.org/10.1017/S0950268816002120

Pestova, T. v., & Hellen, C. U. T. (2021). Translation | Translation initiation in eukaryotes: Factors and mechanisms. In *Encyclopedia of Biological Chemistry: Third Edition* (Vol. 4). https://doi.org/10.1016/B978-0-12-819460-7.00631-9

Que, X., Svärd, S. G., Meng, T. C., Hetsko, M. L., Aley, S. B., & Gillin, F. D. (1996). Developmentally regulated transcripts and evidence of differential mRNA processing in Giardia lamblia. *Molecular and Biochemical Parasitology*, *81*(1). https://doi.org/10.1016/0166-6851(96)02698-9

Querido, J. B., Sokabe, M., Kraatz, S., Gordiyenko, Y., Skehel, J. M., Fraser, C. S., & Ramakrishnan, V. (2020). Structure of a human 48S translational initiation complex. *Science*, *369*(6508). https://doi.org/10.1126/SCIENCE.ABA4904

Rao, V. S., Srinivas, K., Sujini, G. N., & Kumar, G. N. S. (2014). Protein-Protein Interaction Detection: Methods and Analysis. *International Journal of Proteomics*, *2014*. https://doi.org/10.1155/2014/147648

Rodnina, M. v. (2018). Translation in prokaryotes. In *Cold Spring Harbor Perspectives in Biology* (Vol. 10, Issue 9). https://doi.org/10.1101/cshperspect.a032664

Rogawski, E. T., Bartelt, L. A., Platts-Mills, J. A., Seidman, J. C., Samie, A., Havt, A., Babji, S., Trigoso, D. R., Qureshi, S., Shakoor, S., Haque, R., Mduma, E., Bajracharya, S., Gaffar, S. M. A., Lima, A. A. M., Kang, G., Kosek, M. N., Ahmed, T., Svensen, E., … Bessong, P. O. (2017). Determinants and impact of Giardia infection in the first 2 years of life in the MAL-ED birth cohort. *Journal of the Pediatric Infectious Diseases Society*, *6*(2). https://doi.org/10.1093/jpids/piw082

Ruffner, H., Bauer, A., & Bouwmeester, T. (2007). Human protein-protein interaction networks and the value for drug discovery. In *Drug Discovery Today* (Vol. 12, Issues 17–18). https://doi.org/10.1016/j.drudis.2007.07.011

Savioli, L., Smith, H., & Thompson, A. (2006). Giardia and Cryptosporidium join the "Neglected Diseases Initiative." *Trends in Parasitology*, *22*(5). https://doi.org/10.1016/j.pt.2006.02.015

Schmitt, E., Coureux, P. D., Kazan, R., Bourgeois, G., Lazennec-Schurdevin, C., & Mechulam, Y. (2020). Recent Advances in Archaeal Translation Initiation. In *Frontiers in Microbiology* (Vol. 11). https://doi.org/10.3389/fmicb.2020.584152

Shine, J., & Dalgarno, L. (1974). The 3' terminal sequence of Escherichia coli 16S ribosomal RNA: complementarity to nonsense triplets and ribosome binding sites. *Proceedings of the National Academy of Sciences of the United States of America*, *71*(4). https://doi.org/10.1073/pnas.71.4.1342

Smith, D. B., & Johnson, K. S. (1988). Single-step purification of polypeptides expressed in Escherichia coli as fusions with glutathione S-transferase. *Gene*, *67*(1). https://doi.org/10.1016/0378-1119(88)90005-4

Spriggs, K. A., Bushell, M., & Willis, A. E. (2010). Translational Regulation of Gene Expression during Conditions of Cell Stress. In *Molecular Cell* (Vol. 40, Issue 2). https://doi.org/10.1016/j.molcel.2010.09.028

Ventura, L. L. A., de Oliveira, D. R., Gomes, M. A., & Torres, M. R. F. (2018). Effect of probiotics on giardiasis. Where are we? In *Brazilian Journal of Pharmaceutical Sciences* (Vol. 54, Issue 2). https://doi.org/10.1590/s2175-97902018000217360

Vikis, H. G., & Guan, K. L. (2004). Glutathione-S-transferase-fusion based assays for studying protein-protein interactions. In *Methods in molecular biology (Clifton, N.J.)* (Vol. 261). https://doi.org/10.1385/1-59259-762-9:175

Walls, D., & Loughran, S. T. (2011). Purification of proteins fused to glutathione S-tranferase. *Methods in Molecular Biology (Clifton, N.J.)*, *681*(3). https://doi.org/10.1007/978-1-60761-913-0

Yang, Y., & Wang, Z. (2019). IRES-mediated cap-independent translation, a path leading to hidden proteome. In *Journal of Molecular Cell Biology* (Vol. 11, Issue 10). https://doi.org/10.1093/jmcb/mjz091

Zhang, A. (2009). Protein interaction networks: Computational analysis. In *Protein Interaction Networks Computational Analysis* (Vol. 9780521888950). https://doi.org/10.1017/CBO9780511626593

Zheng, X., Hu, G. Q., She, Z. S., & Zhu, H. (2011). Leaderless genes in bacteria: Clue to the evolution of translation initiation mechanisms in prokaryotes. *BMC Genomics*, *12*. https://doi.org/10.1186/1471-2164-12-361

VITA

Francis Owusu Kwarteng was born on September 11, 1995. He attained his High School Diploma in general science from Opoku Ware School in Kumasi, Ghana, in June 2014. He was enrolled at the University of Cape Coast, where he graduated with his bachelor's degree in Medical Laboratory Science in 2019. He enrolled at the University of Louisiana Monroe in 2021 and received a Master of Science in Biology in May 2023.